Design, Analysis and Testing of a PRSEUS Pressure Cube to Investigate Assembly Joints

Nicolette Yovanof[*], Andrew E. Lovejoy[†], Jaime Baraja[‡], and Kevin Gould[§]

Due to its potential to significantly increase fuel efficiency, the current focus of NASA's Environmentally Responsible Aviation Program is the hybrid wing body (HWB) aircraft. Due to the complex load condition that exists in HWB structure, as compared to traditional aircraft configurations, light-weight, cost-effective and manufacturable structural concepts are required to enable the HWB. The Pultruded Rod Stitched Efficient Unitized Structure (PRSEUS) concept is one such structural concept. A building block approach for technology development of the PRSEUS concept is being conducted. As part of this approach, a PRSEUS pressure cube was developed as a risk reduction test article to examine a new integral cap joint concept. This paper describes the design, analysis and testing of the PRSEUS pressure cube test article. The pressure cube was required to withstand a 2P, 18.4 psi, overpressure load requirement. The pristine pressure cube was tested to 2.2P with no catastrophic failure. After the addition of barely visible impact damage, the cube was pressure loaded to 48 psi where catastrophic failure occurred, meeting the scale-up requirement. Comparison of pretest and posttest analyses with the cube test response agree well, and indicate that current analysis methods can be used to accurately analyze PRSEUS structure for initial failure response.

Introduction

The current focus of NASA's Environmentally Responsible Aviation Program (ERA) is the hybrid wing body (HWB) vehicle, which was chosen for its potential to demonstrate significantly increased fuel efficiency of high-lift aircraft. A HWB aircraft employs advanced technologies to achieve a highly integrated airframe that is capable of substantial aerodynamic performance improvements, resulting in reduced fuel burn and pollutants compared to today's aircraft.[1] The key structural challenge of a HWB aircraft is the ability to create a cost- and weight-efficient, non-circular, pressurized shell. Airframe weights are kept low through the extensive use of advanced composite materials, resulting in architectures that are appreciably lighter than comparable aluminum designs.

Global analysis of a HWB vehicle reveals that the majority of the structural panels are subjected to high loading in both the span-wise and chord-wise directions, in addition to the internal cabin pressure that is reacted through panel bending (Fig. 1). This differs from a conventional round fuselage section that reacts cabin pressure by hoop tension. The design, analysis, and testing of these nearly flat pressurized panels requires more assessment than traditional vehicles. The fuselage of a HWB aircraft must meet the overpressure case of 2P, 18.4 psi, where 1P is defined at limit load as 9.2 psi. Preliminary analysis and testing show that with

[*] Analysis Engineer, The Boeing Company, Boeing Research & Technology, 2600 Westminster Avenue, Seal Beach, CA, 90740, MC: 110-SK56, Nicolette.P.Yovanof@Boeing.com.
[†] Research Aerospace Engineer, NASA Langley Research Center, Structural Mechanics & Concepts Branch, MS 190, Hampton, VA, 23681.
[‡] Design Engineer, The Boeing Company, Boeing Research & Technology, 2600 Westminster Avenue, Seal Beach, CA, 90740, MC: 110-SK56.
[§] Research Scientist, Analytical Services & Materials, Inc, 107 Research Drive, Hampton, VA, 23666.

the highly integrated structural concept and uninterrupted load paths of the novel baseline architecture, Pultruded Rod Stitched Efficient Unitized Structure (PRSEUS), the internal pressure loading requirements of the HWB fuselage can successfully be met. This paper summarizes the analysis and testing of a risk reduction test article investigating the design, analysis, and testing of the joints for an assembled subscale PRSEUS specimen under pressure.

PRSEUS Concept

In order to close the design on the HWB with a light-weight, cost-effective, manufacturable concept, the PRSEUS configuration shown in Fig. 2 was selected. Trade studies and previous stitching studies indicate that significant weight savings can be achieved through the use of PRSEUS technology.[2-12] PRSEUS is an integral panel assembly produced without an autoclave. PRSEUS uses dry warp-knit fabric materials stitched together to create a preform of the full structural panel, so that all materials can be co-cured with minimal use of inner moldline tooling. Skins, flanges, and webs are composed of layers of graphite material forms that are pre-knitted into multi-ply stacks of Hercules, Inc. AS4 fibers. Several stacks of the warp-knit material are used to build up the desired part thickness and configuration. To maintain the panel geometry during fabrication, first stiffeners (frames and stringers) and then the skin are placed in a stitching tool for assembly prior to moving to a curing tool for resin infusion and consolidation in an oven. Structures are stitched together using Vectran thread. Stiffener flanges are stitched to the skin and no mechanical fasteners are used for joining. Stringers, the stiffeners running in the axial direction, consist of webs with a bulb of unidirectional, pultruded carbon fiber rods at the top of the web. AS4 carbon fiber overwraps surround the bulb. Frame stiffeners, running in the lateral direction, are foam filled hats. In current PRSEUS construction, the pultruded rods are Toray unidirectional T800 fiber with a 3900-2B resin, and the frame stiffeners are filled with Rohacell foam. The warp-knit stacks, used in the PRSEUS skin and stiffeners, uses a (44/44/12) fiber architecture, where the values are percentages of (0/±45/90) degree plies. The nominal stack thickness is 0.052 inches. The panel is infused with HexFlow VRM 34 resin.[2] In the current HWB design, the 44% 0-degree orientation of the fuselage skin is parallel to the frames in the aircraft span-wise direction.

An additional benefit of this concept is the damage arresting capability of the stitching. This arresting capability allows the PRSEUS configuration to operate at higher strain levels and further into the post-buckled design regime. In addition to the load path continuity of a unitized panel design, the PRSEUS stiffeners are optimized for fuselage loading with a continuous 0-degree fiber pultruded rod in the stringer cap, and a frame attached directly to the skin for bending capability and to provide an uninterrupted load path. The narrow stringer passes through a slit, or keyhole, in the frame web to minimize loss of stability and optimize load transfer.

Building Block Development

The HWB structural development program uses a building-block approach to design, analyze, build, and test components, as shown in Fig. 3. Evaluation of the effect of pressure on the PRSEUS concept began with the analysis and testing of the pressure panel that is identified in Fig. 3 as the Internal Pressure Box. This pressure panel was a Technology Readiness Level (TRL) 4 activity that demonstrated the capability of the minimum gauge PRSEUS panel to carry the 2P overpressure load,[13] where 9.2 psi is defined as the 1P limit load. This pressure panel was also the first step to building a large-scale test article of a section of a HWB fuselage to be tested under combined axial and pressure loading.

The focus of the current paper is to predict and demonstrate the behavior of the Pressure

Cube, which is a cube assembly made from integral PRSEUS panels that is subjected to pressure loading, as identified in Fig. 3. The pressure cube is an intermediate test article in the building block plan meant to reduce risk for the TRL 5 large-scale test by demonstrating PRSEUS assembly joint concepts under 2P loading. This activity is a joint effort between NASA and Boeing, where Boeing completed design, analysis, manufacturing, and assembly of the test article, and NASA conducted pressure testing at the NASA Langley Research Center Combined Loads Test Systems (COLTS)[14] facility and provided analysis and post-test correlation.

Pressure Panel

The PRSEUS pressure panel was a building-block test article that demonstrated the pressure loading capability of minimum gauge PRSEUS panels.[13] The as-tested panel had 20-inch frame spacing, 6-inch stringer spacing, and a 0.052-inch skin thickness. Figure 4 shows the dimensions of the stringers and frames used in the pressure panel. Analysis was performed using a model with a combination of shell and beam finite elements. Both linear and nonlinear static analyses were conducted. Testing was carried out by bolting the 108- by 48-inch pressure panel to a metallic pressure vessel, as shown in Figure 5, and introducing the pressure load. The pressure vessel opening was 100 x 40 inches, which determined the effective test section dimensions for the pressure panel. External metallic doublers were bonded to the pressure panel around its perimeter, as seen in Figure 5. Also seen in the figure are the external stiffeners that are integral to the doublers along the long edges of the panel, and are coincident with the stringer locations. These external stiffeners provided bending continuity and tied the stringers to the pressure vessel. The panel was bolted to the pressure vessel through the doublers with two rows of fasteners, as seen in Figure 5. Displacements and strains were monitored using a combination of strain gages, digital image correlation and a laser displacement sensor, with details being provided in reference 13. Testing showed that the pristine pressure panel was able to withstand the required 18.4 psi, 2P, internal overpressure loading condition with no evidence of damage. After barely visible impact damage (BVID) was inflicted to a primary load-carrying member, the rod region of a stringer, the panel was still able to withstand the required 2P load condition, and supported 28.44 psi prior to initial failure through the center stiffener. Damage was arrested by stitching before reaching the skin, and the panel was then loaded to 30 psi without additional damage growth or loss of pressure. Initial failure at 28.44 psi occurred at a load significantly higher than required for commercial transport aircraft, demonstrating that pressure loading is not a critical load condition for a minimum gauge PRSEUS panel. Therefore, the minimum gauge panel geometry of the pressure panel was applied to subsequent panels used for constructing the pressure cube test article.

Pressure Cube

Design

The PRSEUS pressure cube, shown in Fig. 6, consists of six composite PRSEUS panels assembled using aluminum fittings and a new stitched integral cap joint concept. The pressure cube is designed such that it represents a region of the HWB pressurized fuselage section incorporating the cover skin, two side ribs, two side bulkheads, and a pressurized floor section as shown in Fig. 6. The upper panel is representative of the upper cover panel of the baseline aircraft in the pressure cabin region. A feature of its design is that there are few fasteners

protruding through the outer mold line (OML) of the panel that is exposed to the airstream. The sides of the pressure cube are two pairs of opposing panels, arranged symmetrically, that represent rib and bulkhead panel regions. The rib and bulkhead panels are representative of the outer cabin pressure-carrying ribs and the rear pressure bulkhead of the baseline aircraft, respectively. The floor panel is not strictly representative of the baseline aircraft because of the access door and instrumentation pass-through, but for convenience it was designed to use available panel tooling.

There are stitched T-shaped integral caps manufactured into the panels that reduce the complexity and number of metallic fittings required to assemble the panels together. The integral cap joint design is the primary focus of the pressure cube risk reduction test article. As the first test specimen where PRSEUS panels have been joined together to create a 90-degree corner, the primary purpose of the pressure cube test was to verify that the joint concept could hold the adjusted 2P load case that would be scaled up to account for the subscale cube dimensions. Integral cap members are incorporated around all four edges of the crown panel to provide a means of attaching the cube side panels (Fig. 6). The rib panels incorporate integral flanges to provide a means of attachment to the bulkhead panels. The bulkhead panels have only one cap at the lower end where they interface with the floor panel.

Assembly

Assembly began by performing a fit check with all six panels in hand. The use of Determinant Assembly "DA" holes, three (3) per side on each of the cube's cap flanges, became very useful to do fit checks without the need of any assembly tooling. During the initial fit check, findings were discovered and recorded to determine gaps, shimming, and panel to panel riding conditions. The cube was assembled in sequence by first fastening the panels together at the caps before installing the metallic fittings. The typical fastener was a titanium ¼-inch diameter lockbolt and it was wet installed to prevent any pressure leaks. The cube was sealed internally at the caps and joints without the need of any faying surface application for this cube specimen. The last step prior to packaging the cube assembly for shipping was to apply a coat of flat white-gray paint on the OML of the crown panel, two of the side panels, and the floor panel. This white coat was applied to help visualize the path of panel delamination and cracks during pressure testing at NASA.

Analysis

A detailed finite element model (FEM) was used to obtain linear analysis predictions and nonlinear analysis verification. Detailed local FEMs were created for joint analysis, and when necessary, additional analysis codes were used to predict the response of specific local regions of the cube. Detailed analysis was required to predict the failure loads of the PRSEUS pressure cube and to verify the analysis methods that will be used for design and analysis of the large-scale test article. Linear analysis was completed prior to testing in order to determine the panel strains and displacements for correlations during the test, to predict the critical panel locations and failure modes, and to demonstrate that the overall specimen strength meets the 2P load requirements.

Modeling

The global FEM was developed for use with MSC/Nastran,[15] and comprises six panels (crown, floor, two bulkhead, and two rib panels), aluminum fittings, and titanium bolts. Each panel includes sufficient details to represent the skin, stringers, frames, and T-section caps. One-

dimensional bar elements were used in modeling the "stringer bulbs," which contain the pultruded rod and the wrap around the rod. Two-dimensional shell elements were used in modeling skins, stringer flanges and webs, T-section caps, frame webs, and aluminum fittings. Three-dimensional solid elements were used to model the frame foam cores. The titanium fasteners were modeled using Nastran CFAST fastener connector elements. There are a total of 253,575 nodes, 279,056 shell and beam elements, and 2,144 fastener connector elements in the global FEM (see Fig. 8). More than one fastener connector element is needed when joining more than two plates together, resulting in the number of fastener connector elements being nearly double the actual number of bolts used in the cube assembly.

Detailed analysis of the local joints was completed using a 3-D local FEM with P-Elements using StressCheck[16] and Nastran to assess the interlaminar tension and shear capabilities of the PRSEUS integral cap joint. When the cube is loaded with internal pressure, the bending loads on ribs and bulkheads transfer to the top and floor panels through the T-section caps. As a result, these T-section caps are subjected to both pull-off loads and bending moments, and therefore experience high interlaminar tension and shear stresses along the fillets.

Pretest Analysis Results

Pretest analysis results were compiled to determine if the cube design satisfied the requirements, to assist in determining test instrumentation, and to provide predictions for monitoring of the testing. The detailed assessment of the joint shows that the lowest margin-of-safety is interlaminar tension at the interface of the inner radius of the rib integral cap, as shown in Fig. 9. This minimum joint margin as predicted by the FEM-based StressCheck analysis does not become critical (zero) until the cube is loaded beyond 2P, at a pressure of approximately 20 psi (Fig 9a). In a more detailed Nastran FEM-based analysis, the preliminary failure in the joint occurs at 16 psi, which is still above the required 1.5P limit load for initial damage growth (Fig 9b).

The global model linear results indicated that the pressure cube experienced damage growth at locations other than joints starting at 28.5 psi with local resin failure at the frame web keyholes. As local failures continue, the next major critical margin is for the metallic fitting connecting the crown frame to the rib frame, which was predicted to reach yield strength at 32.4 psi and ultimate failure strength at 37 psi. Frame fitting stress margins were calculated by scaling the linear analysis FEM results shown in Fig. 10 for a pressure of 18.4 psi.

After the test, the analyses and associated assumptions were revisited, including geometric nonlinear behavior. The global finite element model used for the pretest analysis was also used for the post-test analysis, but for post-test analysis, geometrically nonlinear analysis was performed using Nastran. The analysis used linear elastic material properties, and was carried out to a pressure of 50 psi. Since this was a global analysis only, details such as strains around keyholes or bolt locations are not accurately predicted by this analysis. The nonlinear analysis displacement contours at 28.5 psi are shown in Fig. 11. The maximum difference between the linear and nonlinear displacements of the cube occurs in the skin and is approximately 17%. This difference is due to the deflected shape being more efficient that the flat-sided linear FEM results. However, the linear and nonlinear displacements at the stringers and frames are nearly identical, indicating that the response at the stiffeners is linear in nature, a response that was observed in the pressure panel analysis and test.[13] The primary focus of the post-test analysis was to examine the metal fittings. Figure 12 shows the stress contours for the crown-to-rib frame fittings. The nonlinear analysis indicates that these fittings will reach the ultimate failure stress of 80 ksi at around 47.5 psi pressure load.

The validation of analysis methods and capabilities through testing is an additional focus of this task. The initial global analysis and sizing of the HWB aircraft indicates that the PRSEUS configuration is sufficiently light to meet the minimum weight required for the concept. The detailed specimen analysis supports this theory. The panel meets the 2P loading requirements in the global FEM analysis. The initial test predictions support the global optimization results that show that the PRSEUS minimum gauge panel concept can meet the pressure loading requirements.

Testing

The pressure cube was tested in the NASA Langley Research Center COLTS facility in August of 2011. Preliminary tests were completed up to 1P to do an instrumentation check. The first test was a pressurizing of the pristine cube up to 2P. Once the 2P test was complete, data was reviewed, and NDI taken. The pressure cube was then impacted with BVID and pressurized to failure.

Test Set-up

The test set-up for the pressure cube is shown in Figure 13. The pressure cube was instrumented with 11 direct current displacement transducers (DCDTs) and 168 strain gages. The locations of all DCDTs and selected strain gages for which results are reported are described in Tables 1 and 2, respectively, and are shown in Figures 14 and 15, respectively. A video digital image correlation system,[17] VIC-3D[18] (hereafter referred to as VIC), was used to monitor displacements and strains on two exterior sides of the pressure cube, one rib panel and one bulkhead panel. Two VIC systems were used for global measurements, and a third system was added in the final load-to-failure test to monitor a local region in the vicinity of barely visible impact damage (BVID). Additionally, video monitoring of the interior of the pressure cube was carried out using video cameras with light-emitting diode (LED) lighting, and several cameras provided video monitoring of the exterior of the pressure cube. Complete details of the test set-up can be found in reference 19.

Test Procedure

The pressure cube was subjected to several pressure loads at various levels in the pristine condition, and was pressure loaded to failure with BVID imparted to the exterior of the cube at a rib integral cap web location. Design pressures for the cube are designated as 1P, which represents the normal operating pressure of 9.2 psi, and 2P, which represents the 18.4 psi maximum overpressure condition. In the pristine condition, two check-out tests were conducted with the pressure ramped up to 4.6 psi (0.5P). These check-out tests were used to verify proper operation of all data acquisition systems and the pressure control system. The pristine cube was then cycled up to 1P pressure and then completely unpressurized. The final pristine cube test cycled the pressure up to 20.15 psi (2.2P) prior to being unpressurized. The purpose of the 2.2P load is to ensure that no failure will occur for the overpressure condition, but with an additional margin of 10% included. At the conclusion of the pristine cube tests, the cube was examined using ultrasonic NDI and BVID was introduced. The cube was turned on its side, NDI was performed, then BVID was imparted to the rib integral cap web that attached the rib and bulkhead that were monitored using the VIC systems, as shown in Figure 16. The location of the BVID with respect to the integral cap web is shown in Figure 17, and its location on the cube is shown in Figure 18. The BVID was imparted using a drop weight impactor with an impact energy of 100 ft-lbs with a 1-inch spherical impactor. Figure 19 shows the impact location before

and after introducing the BVID. Additional NDI was performed in the vicinity of the BVID with the cube on its side prior to being rotated back to the test position and reinstalling DCDTs. The pressure cube was then pressurized until catastrophic failure occurred. NDI was performed on what remained of the cube after the catastrophic failure.

Test Data

As described in the test set-up section, data was collected on the pressure cube using DCDTs, strain gages and VIC. Data was collected for all test loads; the two check-out tests, the 1P test, the 2.2P test and the test to failure. Ref. 20 gives all of the pressure cube test data and a discussion of the response for all five of the test loads. The two check-out tests were uneventful, as was expected since the load level was low. The third loading took the pressure cube to 1P, and the maximum center-of-panel displacement measured by the DCDTs for the crown, rib and bulkhead were 0.042, 0.0098 and 0.19 inches, respectively. The only strain gage that showed other than smooth response was SG95AW, as shown in Figure 20. As shown in Table 2, this gage is above a keyhole, and this discontinuity could be attributed to cracking or failure of the resin that collects between the stringer and integral cap web during infusion. The stringers are expected to pass through keyholes without any connection, but resin collects in the keyhole region providing a weak connection between the stringer and structure in which the keyhole exists (i.e. frame, integral cap). Therefore, testing showed no unexpected response up to 1P.

The cube was then loaded to 2.2P. No catastrophic failure or visible damage resulted from the 2.2P loading. However, test data indicates that nonvisible damage did occur. DCDT6 showed two significant discontinuities in displacement at about 16 and 19 psi, as shown in Figure 21. The strain gages in the vicinity of DCDT6 show discontinuities at the same pressure levels, as shown in Figures 22-24. Also, similar behavior is seen at gages in the mirroring locations, as shown in Figures 25-27. Numerous other gages showed mildly nonlinear behavior and tiny discontinuities in strain level, but they were not as severe as those shown in the figures. NDI was performed only on the crown panel after the 2P test. The ultrasonic NDI indicated that delaminations developed in the vicinity of the crown integral caps attached to the ribs, as shown in Figure 28, which is consistent with the DCDT and strain gage data that was presented. Therefore, no visible damage was observed, but there was internal, nonvisible damage after the 2.2P load.

Lastly, the pressure cube was loaded to catastrophic failure after BVID was introduced. Throughout the loading, many indications of local damage were observed by the DCDTs and strain gages, but no visible damage was observed, and catastrophic failure did not occur until 48 psi. Displacement plots for selected DCDTs are shown in Figures 29-32, and the VIC-measured displacements just prior to catastrophic failure are shown in Figures 33 and 34 for the rib and bulkhead, respectively. The maximum strains observed were on the bulkhead frame in the vicinity of a keyhole and on the cap, as shown in Figures 35-36. In the vicinity of the keyhole, the strain instantaneously increased from -4,000 με to -12,000 με at 45.7 psi for SG83BW, and from -5,000 με to -12,000 με from 47 to 48 psi for SG75BW. However, at the keyhole, local failures would be expected due to the stress concentration, but may not necessarily lead to catastrophic failure. The maximum strains in the frame caps were approximately -10,000 με, as seen in Figures 37 and 38. The pressure cube after failure is shown in Figure 39. In addition to the composite failure, failure in the aluminum connection between the crown panel and VIC rib frames was found, as shown in Figure 40.

Test/Analysis Correlation

Upon completion of the tests, the data and analysis failure location predictions showed the combined pretest and post-test analytical methods used correlated well with the test results. Assessment of the strain gauge, VIC, and NDI data demonstrated key failure modes and locations were accurately predicted.

The preliminary nonvisible failures in the joint integral cap of the crown panel at 16 and 19 psi were not accurately predicted in the detailed StressCheck model due to inaccurate boundary conditions applied to the local FEMs. In the second analysis using a detailed Nastran model, the failures were predicted to occur at 12.4 psi, which was more conservative than the actual failure load. The conservative prediction was within an allowable load where the stitching could arrest the damage. The second local failure that occurred was at the resin interface at the bulkhead frame keyhole where the stringer passes through. Initial cracking occurred at 20 psi and was not predicted because a detailed assessment of the resin interface was not completed. A third local failure occurred at the bulkhead to rib panel interface where cracking occurred at the noodle interface, the filled region between the cap wrap and the skin, for the rib cap connection to the bulkhead. The analysis predicted failure to occur at 20 psi where the test data shows the first failure at the interface occurred at 22 psi.

Additional local failures occurred between these and the final catastrophic failure at 48 psi, but were not studied in detail in the linear analysis beyond these failures. The next major event predicted to occur was yielding of the metal fitting connecting the crown panel frame to the rib panel frame at a pressure of 37 psi. Fracture of the metallic fitting is suspected to have occurred at 48 psi, leading to the overall catastrophic failure of the specimen. Therefore, the failure load of this fitting was not accurately predicted by linear analysis. However, post-test, nonlinear Nastran analysis indicates that the metal fittings connecting the crown and rib frames will reach ultimate stress at a load of approximately 47.5 psi, which is in very good agreement with the final failure pressure. While the DCDT and strain gages indicate the possibility of numerous local or internal failures occur below 48 psi they did not result in catastrophic failure.

The most likely final failure sequence as indicated by the test results and analysis begins with failure of the metallic splice plates connecting the crown and rib frame. Once the splice plates failed, the detached rib frame would be subjected to increased in-plane bending due to the reduced moment carrying capability, which can result in frame buckling. Frame buckling is supported by the observed damage as shown in Figure 41. After the frame buckles, the load has to redistribute to the adjacent integral cap attaching the rib to the bulkhead, which is incapable of handling the loads, leading to failure of the integral cap. Failure of the integral cap adjacent to the failed frame splice is supported by the fact that when the bulkhead panel blew out, it flew up and away from the VIC rib that had the frame splice failure. The failures in the bulkhead frames that remained in the box can be due to local failures at the keyholes through which the top and bottom stringers pass. Local keyhole failures, such as indicated by the strains shown in Figures 35 and 36, can result in the failure across the frames once the load is redistributed to them after the frame fitting failure and rib frame buckling. The proposed likely final failure sequence is speculative due to the fact that the failure occurred instantaneously and there were no indications by the instrumentation from which to draw clear conclusions, but catastrophic first failure of the frame fitting is supported by the analysis and test data.

As a risk reduction specimen leading to a 30-foot long large-scale test article (see Fig. 6), the loads in the joints of the pressure cube must scale to demonstrate the higher loads in the large-scale test article under the 2P overpressure condition. Additional post-test correlation was done

to relate the bending moments of the pressure cube to those of the large-scale test article. This comparison showed that there is a factor of 2.35 difference in the bending moments due to geometric considerations. Therefore, to scale-up to the large-scale test article bending moment, the pressure cube needed to meet a loading condition of 2.35 times 2P, which is 4.7P, or approximately 43 psi. This scale-up issue demonstrates that the cube failure at 48 psi, 5.2P, correlates to a large-scale test article failure at 20 psi, 2.2P, which meets the 18.4 psi, 2P, overpressure requirement but does not provide excess margin.

Conclusions

The integrated PRSEUS concept meets the necessary requirements of the innovative structural configurations and manufacturing techniques to keep the HWB aircraft cost-effective despite the unconventional airframe geometry and consequential loading of near-flat panels. The risk reduction analysis and testing of an assembled pressure cube is one step along the way to validate the PRSEUS concept in its ability to meet the design needs of a HWB aircraft. In the current study, results indicate that the concept can meet the minimum pressure loading requirements of the pressurized fuselage of a HWB aircraft with near-flat skin panels. Additionally, comparison of analytical results with the cube experimental response agree well, and indicate that current analysis methods can be used to accurately analyze PRSEUS structure and initial failure response. Results from the pressure cube test are being used in preparation for a larger-scale structural test to be conducted under combined loading conditions in the COLTS facility. This capability to withstand the 2P overpressure condition using joined PRSEUS panels is a key element in solving the most critical structural challenges of the HWB concept.

Acknowledgements

The authors wish to thank Marshall Rouse and the staff at the COLTS facility for their efforts in conducting the pressure cube testing.

References

1. Liebeck, R. H., “Design Of The Blended-Wing-Body Subsonic Transport,” 2002 Wright Brothers Lecture, AIAA Paper 2002-0002, August 2002.
2. Velicki, A. 2009. “Damage Arresting Composites for Shaped Vehicles,” NASA CR-2009-215932.
3. NASA TCAT Phase I Study (Novel Blended Wing Body Structural Concepts), Velicki, A., Contract NNL04AA36C CLIN 0001, July 2004.
4. Air Vehicle Technology Integration Program (AVTIP), Delivery Order 0059: Multi-role Bomber Structural Analysis, AFRL-VA-WP-TR-2006-3067, Krishna Hoffman, MAY 2006, Final Report for 14 December 2004 – 08 May 2006, AFRL-VA-WP-TR-2006-3067.
5. Karal, M., “AST Composite Wing Study – Executive Summary,” NASA/CR-2001-210650, Prepared for NASA, Langley Research Center under Contract NAS1-20546, March 2001.
6. Velicki, A. and Thrash, P.J., “Advanced Structural Concept Development Using Stitched Composites,” AIAA Paper 2008-2329, 49th AIAA/ASME/ASCE/SHS/ASC Structures, Structural Dynamics, and Materials Conference, Schaumburg, IL, 7-10 April 2008.
7. Jegley, D., 2010 “Influence of Impact Damage on Carbon-Epoxy Stiffener Crippling,” American Society for Composites meeting, Dayton, OH, Sept 2010.

8. Yovanof, N.P., “Advanced Structural Stability of a Non-Circular BWB-Shaped Vehicle,” 50th AIAA Structures Dynamics and Materials Conference, Palm Springs, CA, May 4-7 2009.

9. Velicki, A., Jegley, D.C., and Thrash P.J., “Airframe Development for the Hybrid Wing Body Aircraft,” AIAA-2009-932, 47th AIAA Sciences Meeting, Orlando, FL, Jan 5-8 2009.

10. Velicki, A., and Thrash P.J., “Blended Wing Body Structural Concept Development,” Aircraft Structural Design Conference, Liverpool, UK, Oct 14-16 2008.

11. Li, V., and Velicki, A., “Advanced PRSEUS Structural Concept Design and Optimization,” AIAA-2008-5840, 12th AIAA/ISSMO Multidisciplinary Analysis and Optimization Conference, Victoria, British Columbia, Canada, Sept. 10-12 2008.

12. Jegley, D.C., Velicki, A., Hansen, D., “Structural Efficiency Of Stitched Rod-stiffened Composite Panels With Stiffener Crippling,” 49th AIAA/ASME/ASCE/SHS/ASC Structures, Structural Dynamics, and Materials Conference, Schaumburg, IL, 7-10 April 2008.

13. Lovejoy, A. E., Rouse, M., Linton, K. A., and Li, V. P., “Pressure Testing of a Minimum Gauge PRSEUS Panel,” AIAA-2011-1813, 52nd AIAA/ASME/ASCE/AHS/ASC Structures, Structural Dynamics and Materials Conference, Denver, Colorado, Apr. 4-7, 2011.

14. Ambur, D. A., Rouse, M., Starnes, J. H., and Shuart, M. J., “Facilities for Combined Loads Testing of Aircraft Structures to Satisfy Structural Technology Development Requirements,” 5th NASA/DoD Advanced Composites Technology Conference, Seattle, WA, August 22-25, 1994.

15. MSC/Nastran 2010, Software Package, MSC.Software Corporation, Santa Ana, CA, 2010.

16. StressCheck, version 8.0, September 2008, Engineering Software Research & Development, Inc, 111 West Port Plaza, Suite 825, St. Louis, MO 63146.

17. McGowan, D. M., Ambur, D. R, and McNeil, S. R., “Full-field Structural Response of Composite Structures: Analysis and Experiment,” AIAA 2003-1623 44th AIAA/ASME/ASCE/AHS Structures, Dynamics and Material Conference, Norfolk, VA, April 2003.

18. Correlated Solutions, Inc., 120 Kaminer Way Parkway Suite A, Columbia, SC 29210 (http://www.correlatedsolutions.com).

19. Lovejoy, A.E., “PRSEUS Pressure Cube Test Data and Response,” NASA TM in preparation.

Table 1: Descriptions of cube DCDT locations.

DCDT	Location
1	Crown panel, centered on frame, centered over integral cap
2	Crown panel, centered on frame, centered over integral cap
3	Crown panel, centered on frame, centered over integral cap
4	Crown panel, centered on frame, centered over integral cap
5	Crown panel, centered on frame, centered over center stringer
6	Crown panel, centered on integral cap, center of crown panel width
7	Crown panel, geometric center of panel
8	Crown panel, centered on center stringer, centered between frame and integral cap
9	Crown panel, centered on center stringer, adjacent to crown panel edge
10	Gray Bulkhead panel, centered between crown and floor panels, centered on bulkhead panel width
11	Gray Rib panel, centered between crown and floor panels, centered on rib panel width

Table 2: Descriptions of cube strain gage locations.

Strain Gage	Location
SG9AS	Crown panel, centered between bulkheads, outer skin adjacent to first stringer flange on gray rib side, parallel to stringer direction
SG9BS	Crown panel, centered between bulkheads, inner skin adjacent to first stringer flange on gray rib side, parallel to stringer direction
SG10AS	Crown panel, centered between bulkheads, outer skin adjacent to first stringer flange on gray rib side, parallel to frame direction
SG10BS	Crown panel, centered between bulkheads, inner skin adjacent to first stringer flange on gray rib side, parallel to frame direction
SG20AS	Crown panel, centered between bulkheads, outer skin adjacent to first stringer flange on VIC rib side, parallel to stringer direction
SG20BS	Crown panel, centered between bulkheads, inner skin adjacent to first stringer flange on VIC rib side, parallel to stringer direction
SG21AS	Crown panel, centered between bulkheads, outer skin adjacent to first stringer flange on VIC rib side, parallel to frame direction
SG21BS	Crown panel, centered between bulkheads, inner skin adjacent to first stringer flange on VIC rib side, parallel to frame direction
SG49BF	Gray rib frame adjacent to VIC bulkhead, centered above stringer 4, top of web inner surface
SG50BF	Gray rib frame adjacent to VIC bulkhead, centered above stringer 4, top of web outer surface
SG55BF	Gray rib frame adjacent to gray bulkhead, centered above stringer 4, top of web inner surface
SG56BF	Gray rib frame adjacent to gray bulkhead, centered above stringer 4, top of web outer surface
SG70AS	Gray bulkhead, centered on frame adjacent to VIC rib and stringer 4, outer skin parallel to frame
SG70BC	Gray bulkhead frame adjacent to VIC rib, centered above stringer 4, top of frame cap
SG75BW	Gray bulkhead frame adjacent to VIC rib, adjacent to bottommost keyhole, 0.3 inches from side of stringer rod, parallel to stringer height
SG77AS	Gray bulkhead, centered on frame adjacent to gray rib and stringer 4, outer skin parallel to frame
SG77BC	Gray bulkhead frame adjacent to gray rib, centered above stringer 4, top of frame cap
SG83BW	Gray bulkhead frame adjacent to gray rib, adjacent to bottommost keyhole, 0.3 inches from side of stringer rod, parallel to stringer height
SG95AW	Rib integral cap web, outer surface, 0.3 inches above top of stringer rod adjacent to keyhole, parallel to rib skin

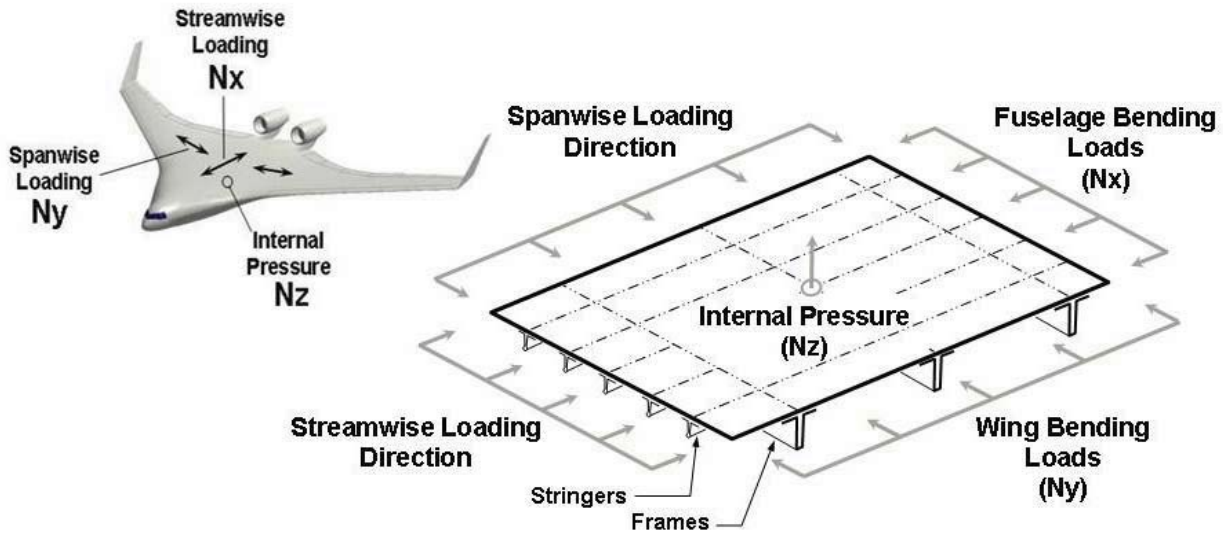

Figure 1. HWB conceptual vehicle and loading patterns.

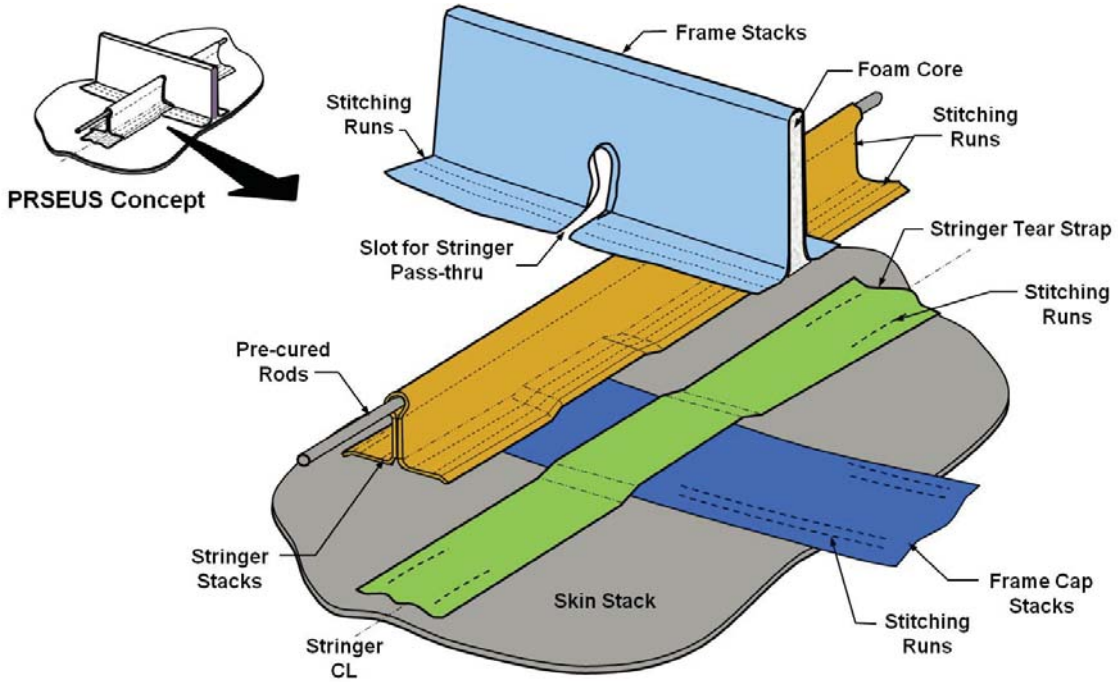

Figure 2. PRSEUS design concept baseline for the HWB.

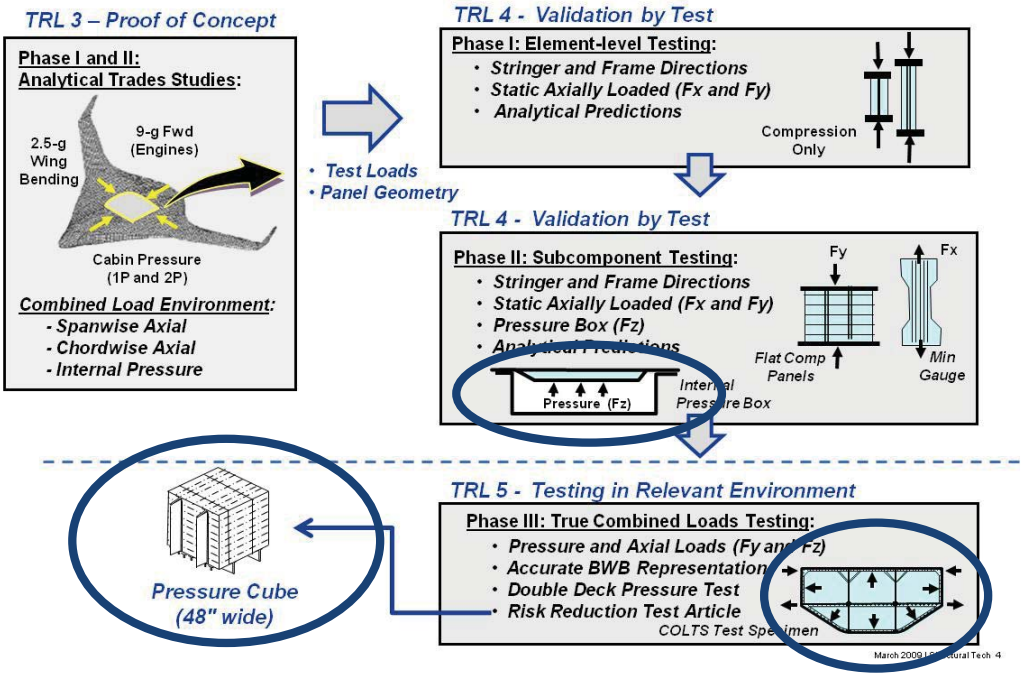

Figure 3. HWB structural development building block approach.

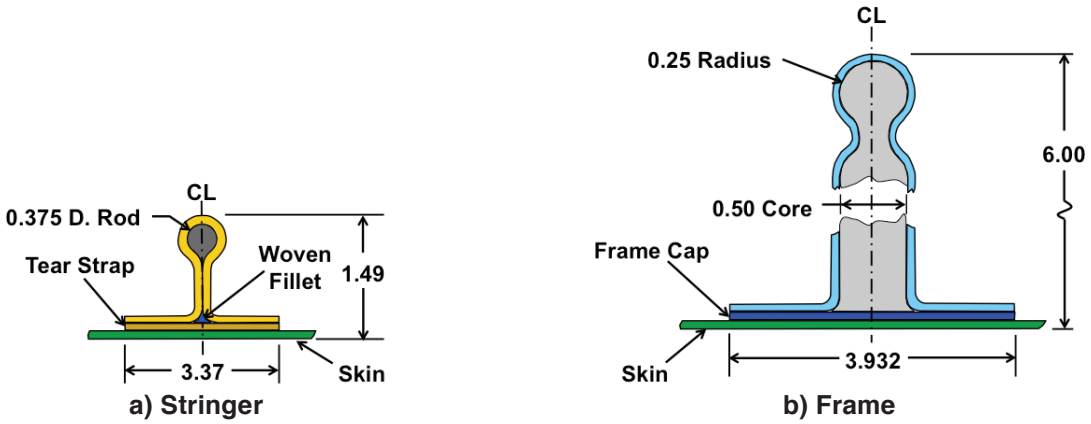

Figure 4. PRSEUS panel stringer and frame cross-sections. Dimensions are in inches.

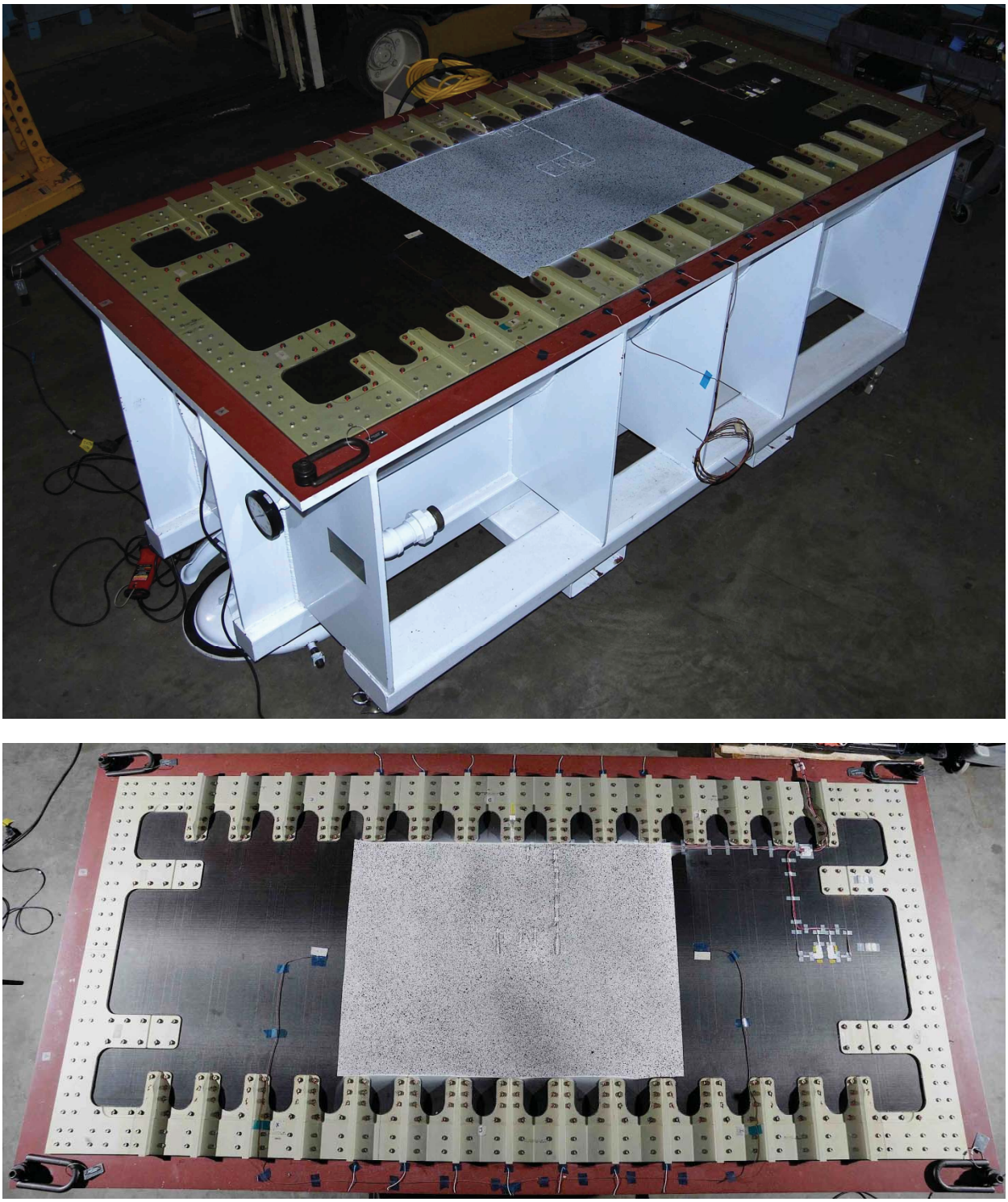

Figure 5. Pressure panel test assembly. Doublers with integral stiffeners are the yellow structure around the perimeter of the panel. The VIC speckle pattern is the white region in the center, and measures approximately 29 by 40 inches.

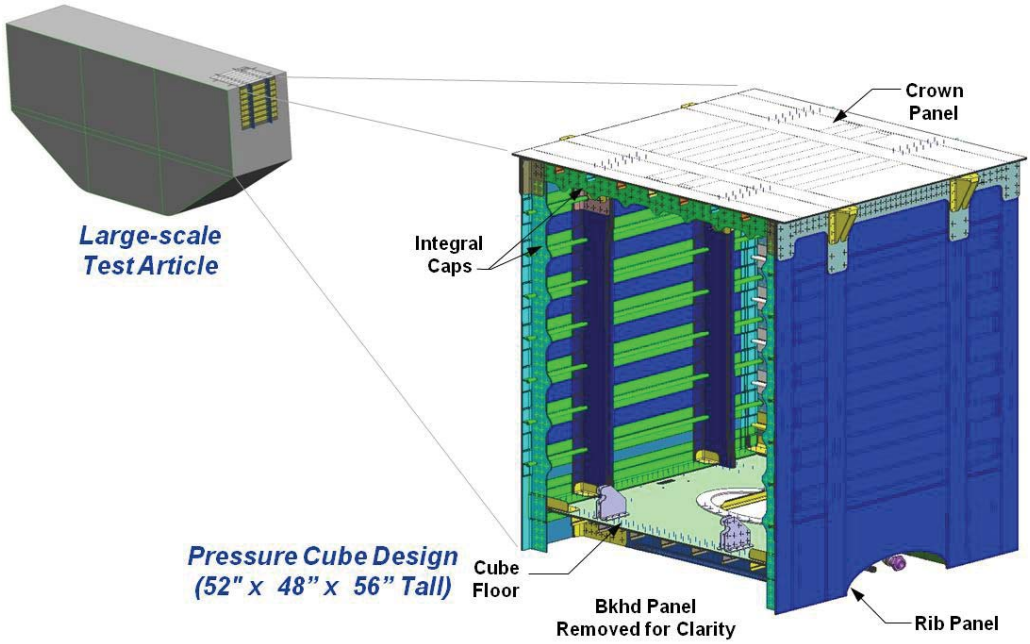

Figure 6. PRSEUS pressure cube is a representative section of the HWB large-scale test article.

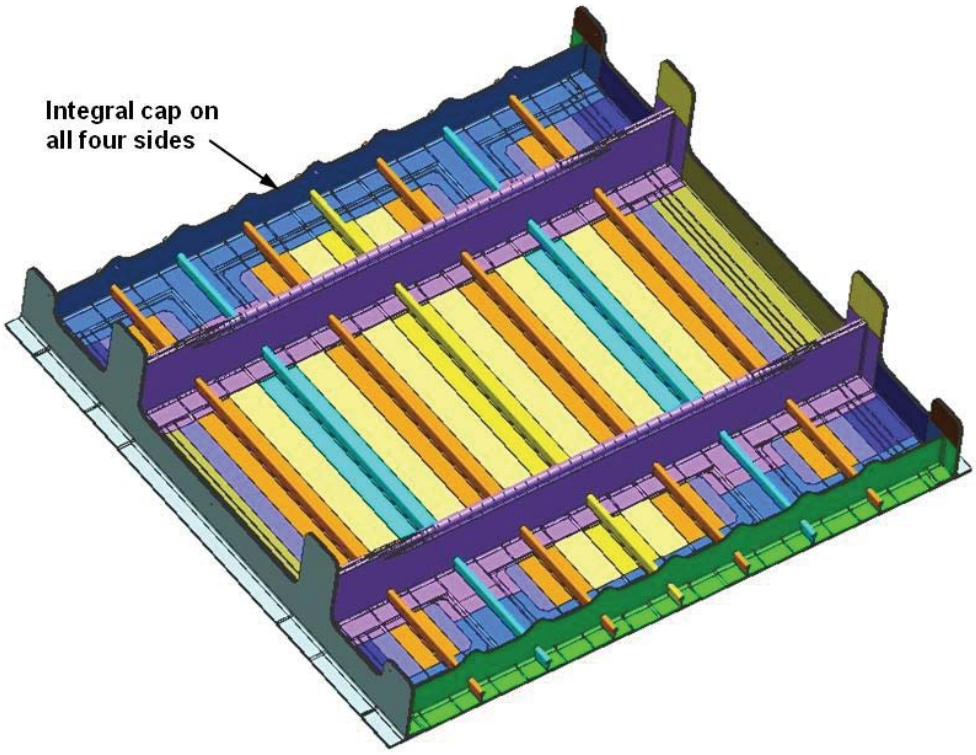

Figure 7. Integral caps on the crown panel demonstrate the new joint design for the PRSEUS panels.

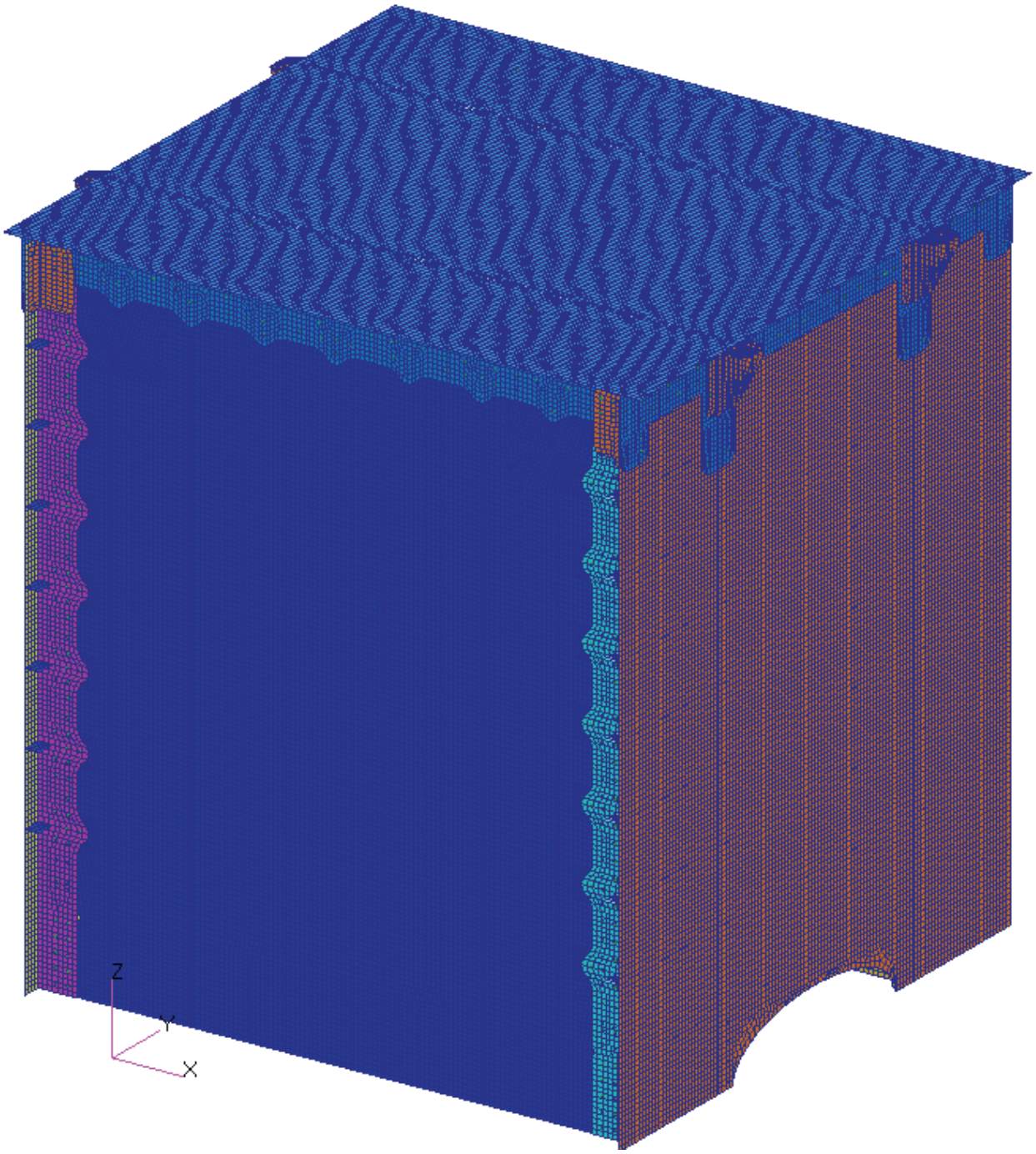

Figure 8. Global FEM comprising 253,575 nodes, 279,056 beam and shell elements, and 2,144 fastener element connections for pressure cube shown in Fig. 6.

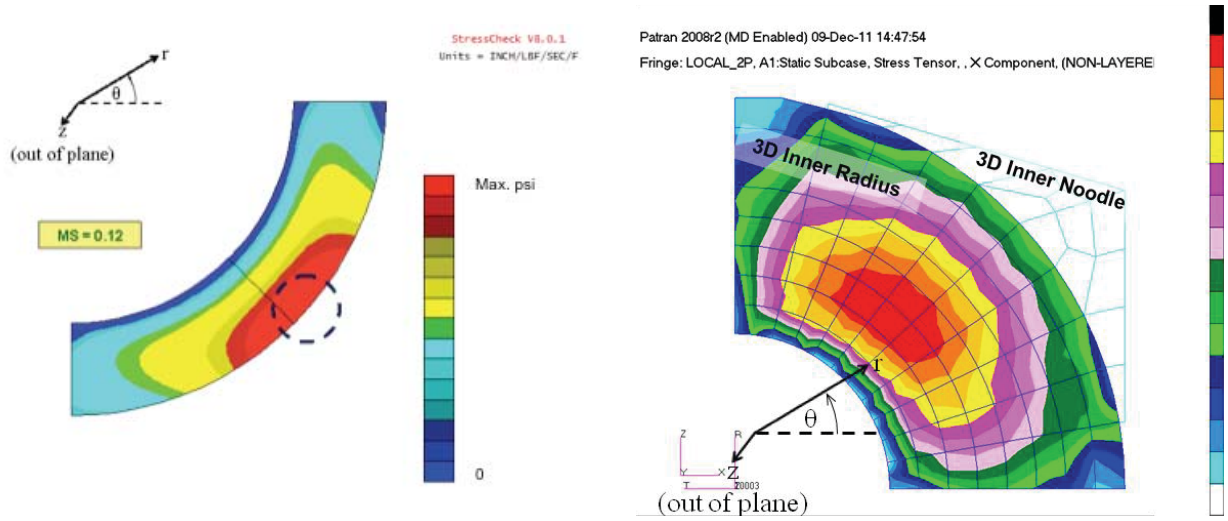

a) StressCheck b) FEM

Figure 9. Pull-off stress contours at the interface of the integral cap showing the predicted failure location

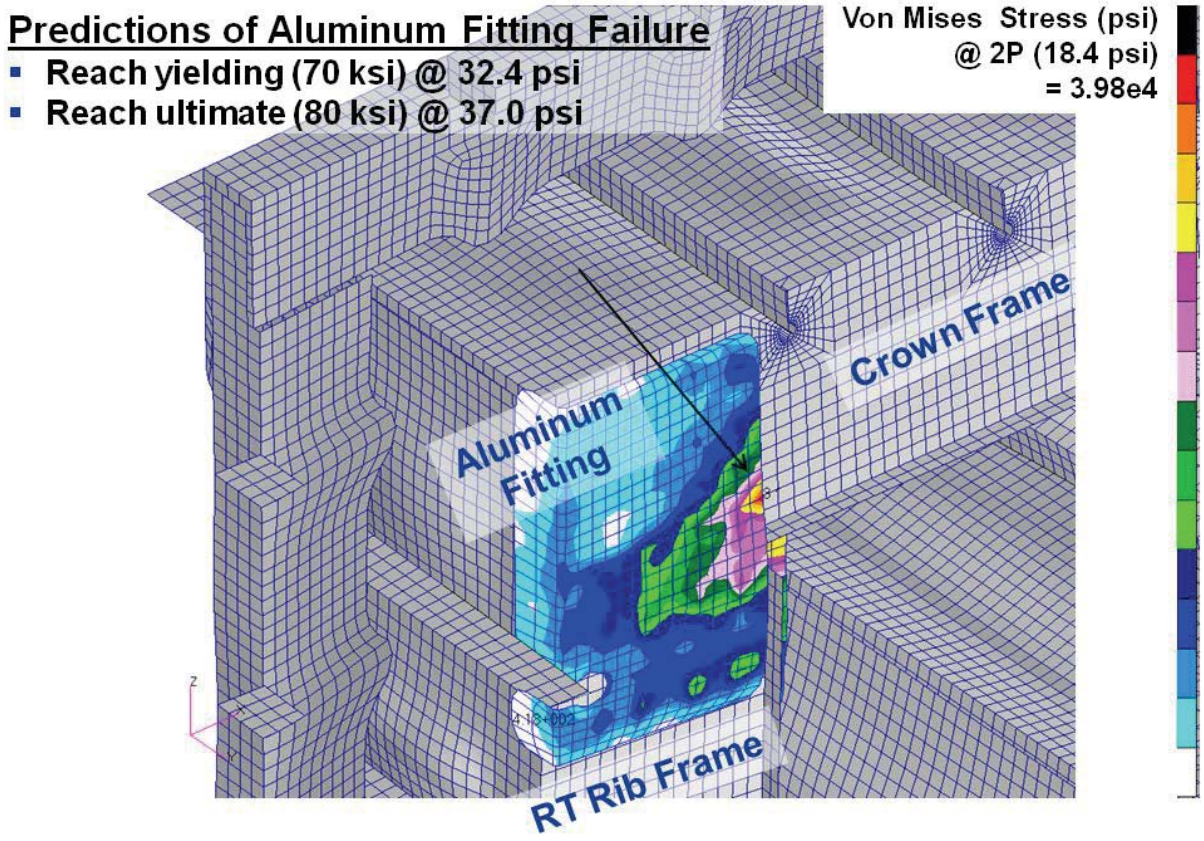

Figure 10. Nastran linear analysis von Mises stresses in metallic crown-to-rib frame fittings at 18.4 psi.

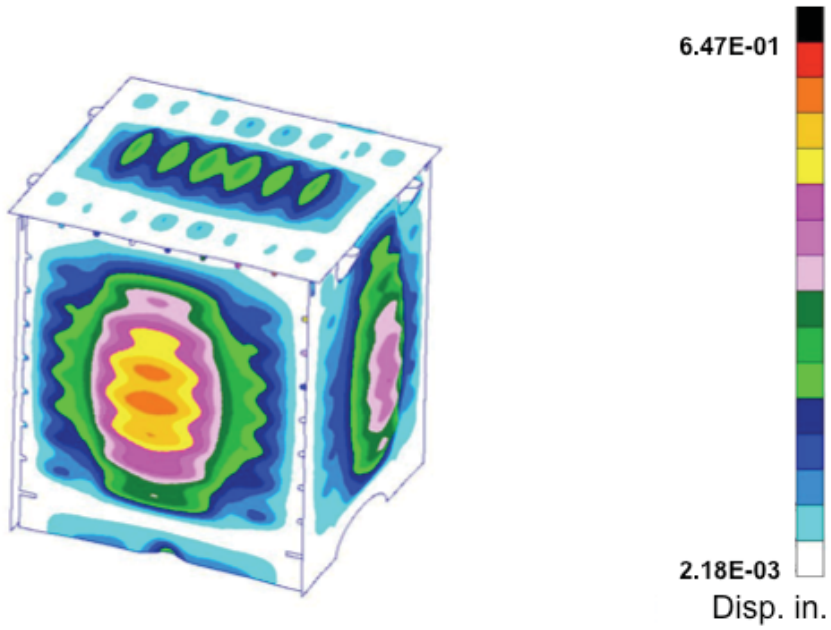

Figure 11. Nastran nonlinear analysis displacement contours at 28.5 psi

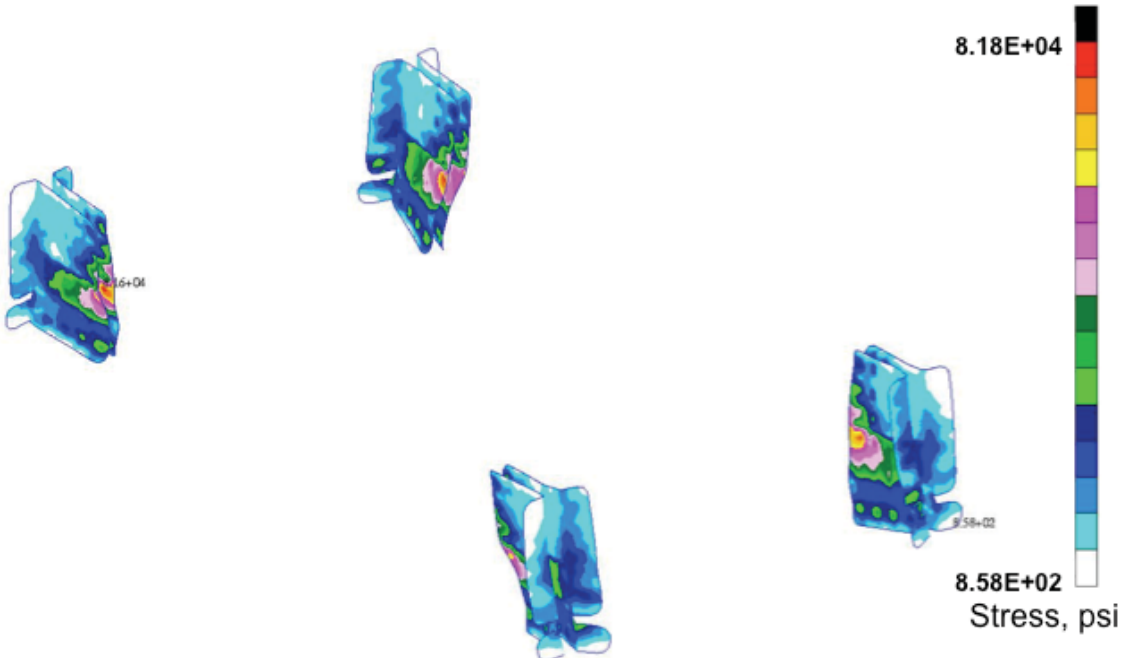

Figure 12. Nastran nonlinear analysis von Mises stresses in crown-to-rib frame fittings at 47.5 psi.

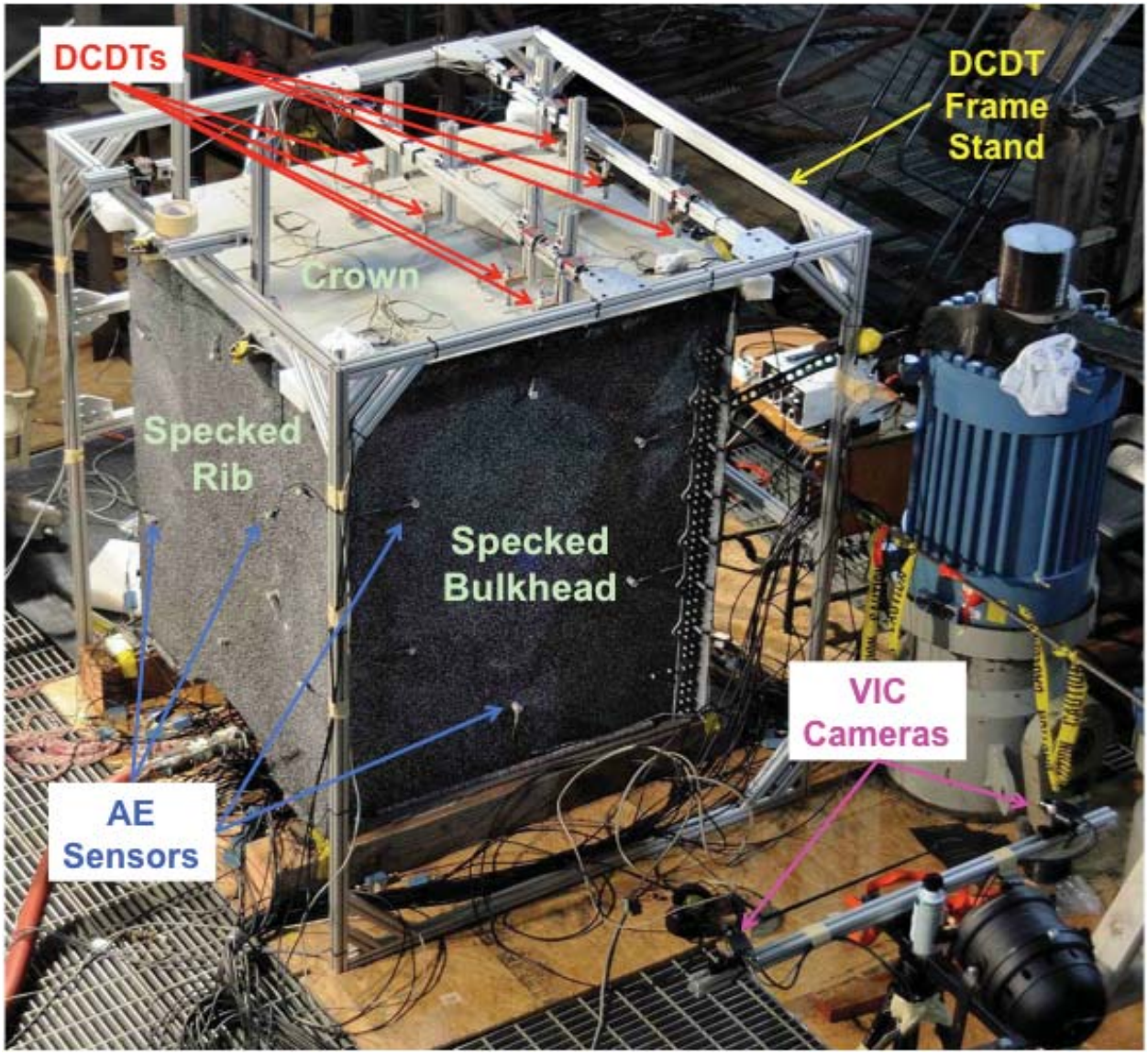

Figure 13. Pressure cube test set-up in the COLTS facility at NASA LaRC.

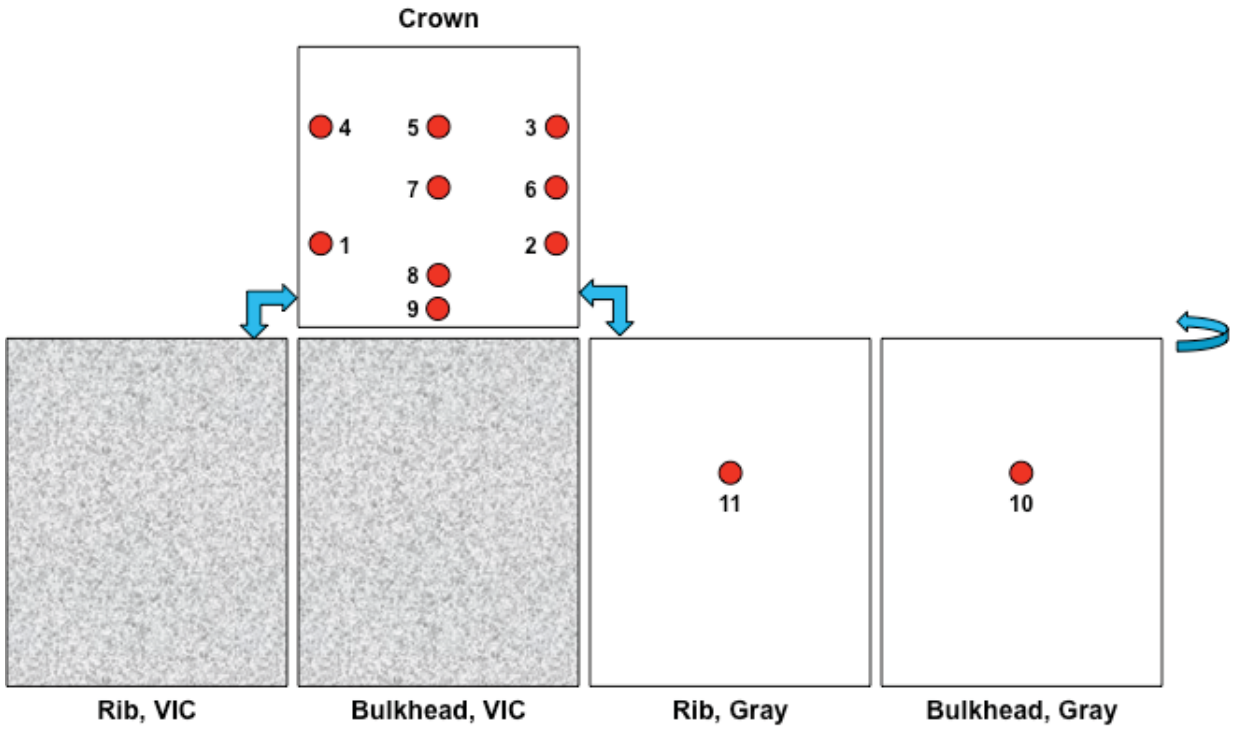

Figure 14. DCDT locations.

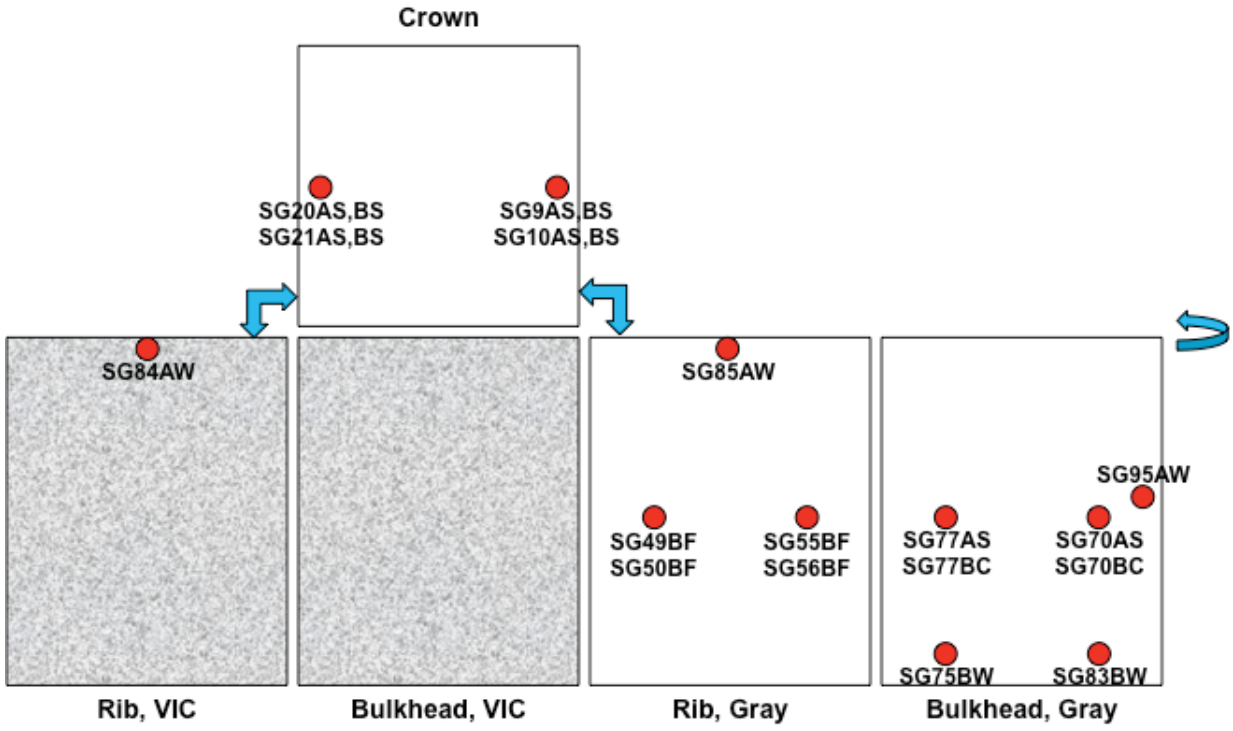

Figure 15. Strain gage locations. Details about locations are presented in table 2.

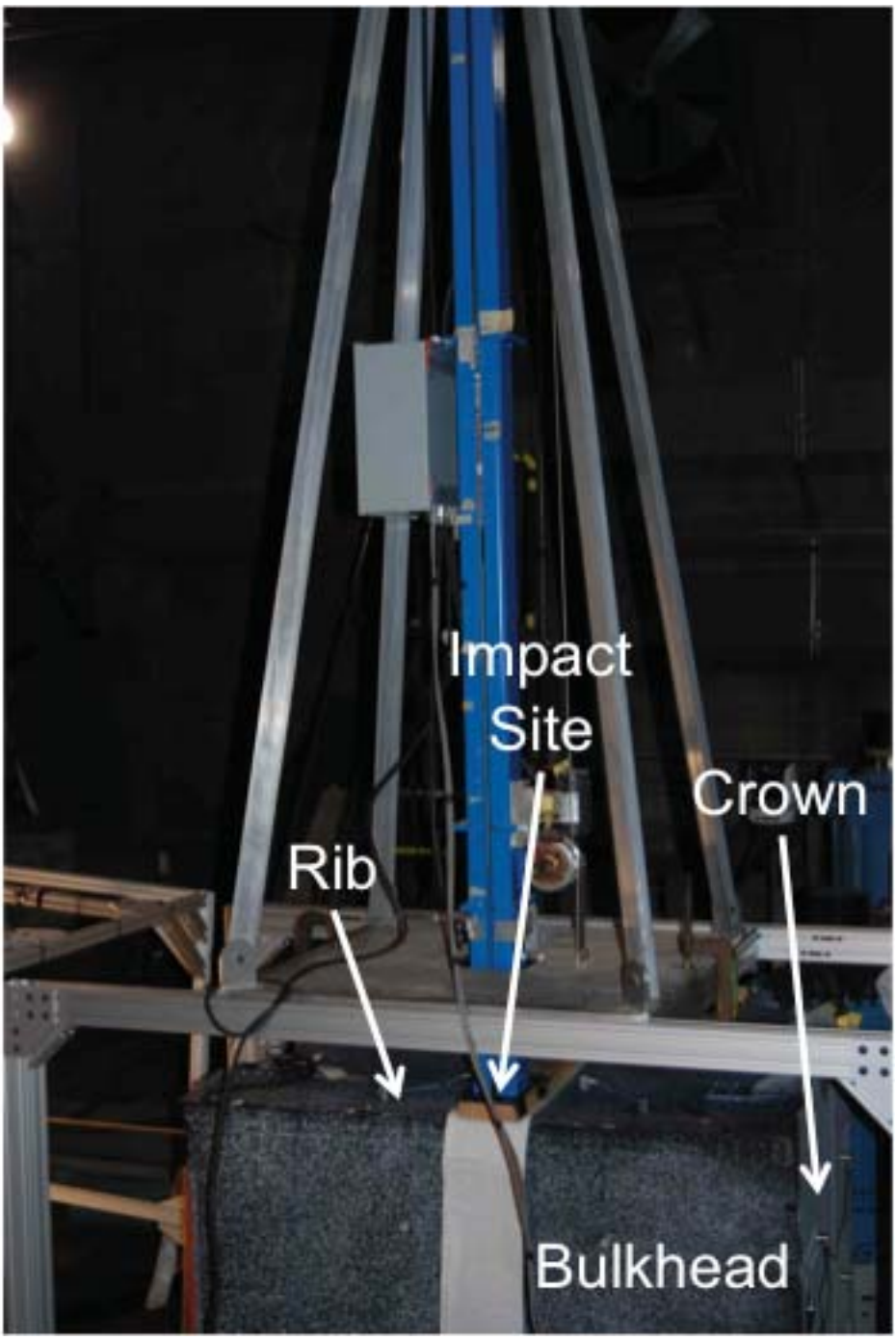

Figure 16. Pressure Cube BVID impact location. (Wood and foam protecting impact site prior to impact.)

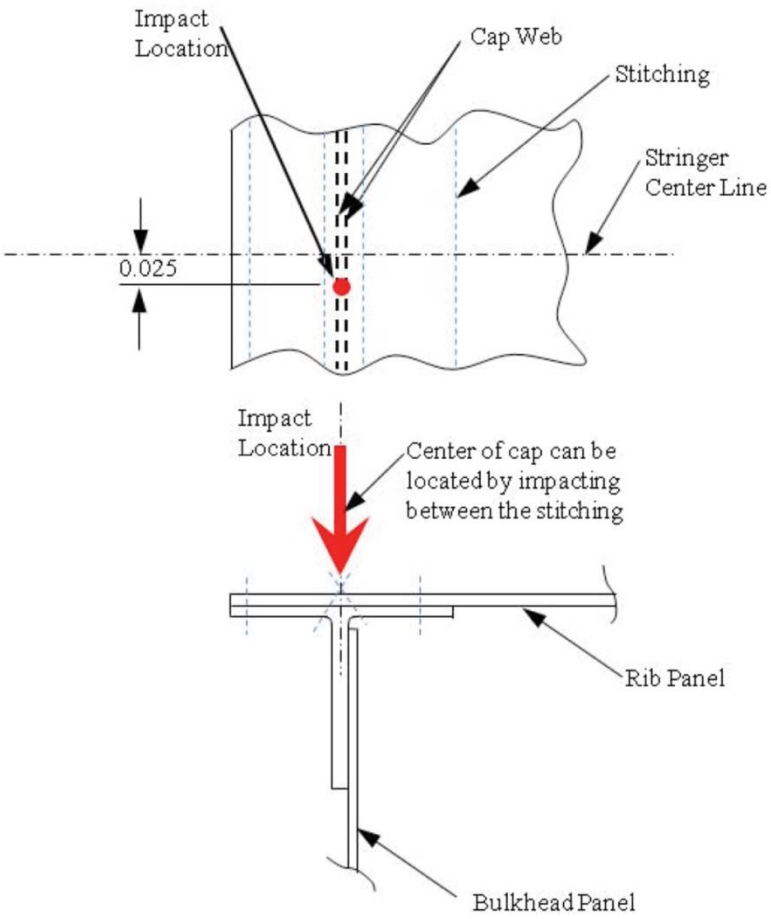

Figure 17. Pressure Cube BVID impact location with respect to integral cap web.

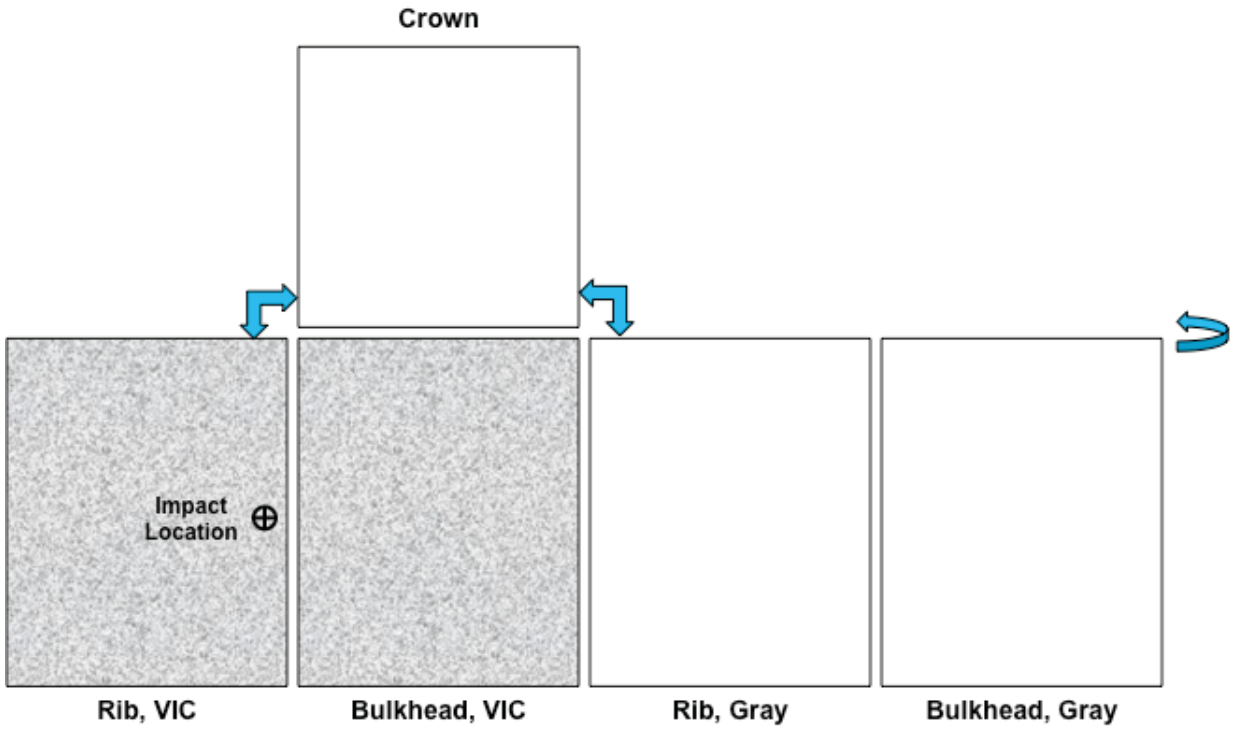

Figure 18. Pressure Cube BVID impact location with respect to cube panels.

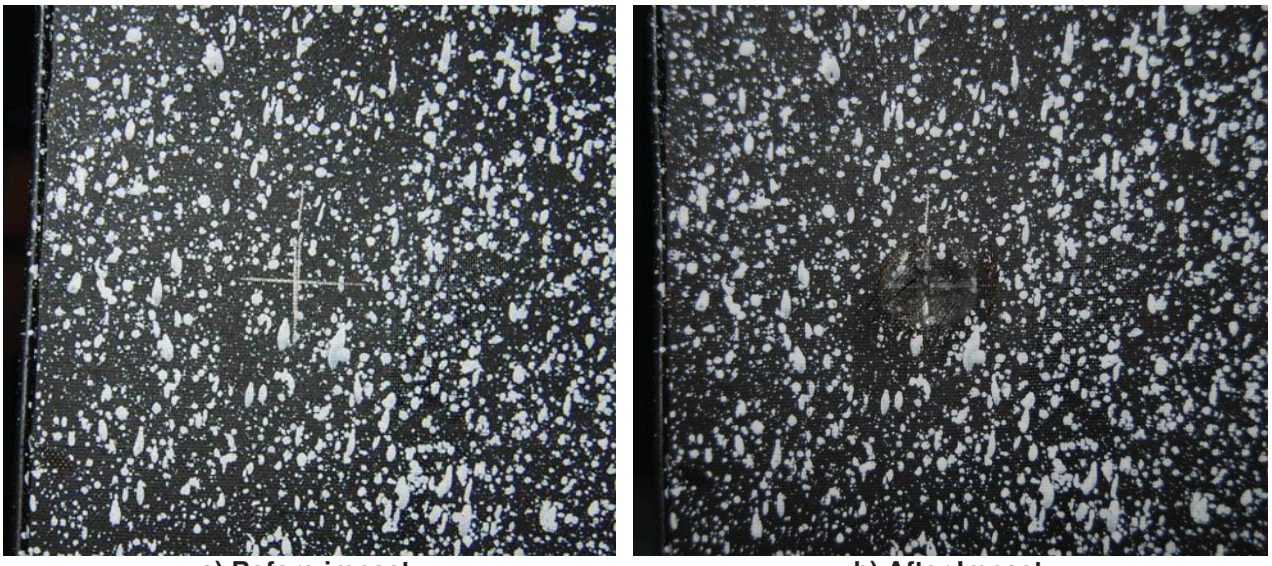

a) Before impact **b) After Impact**

Figure 19. Impact location before and after impact.

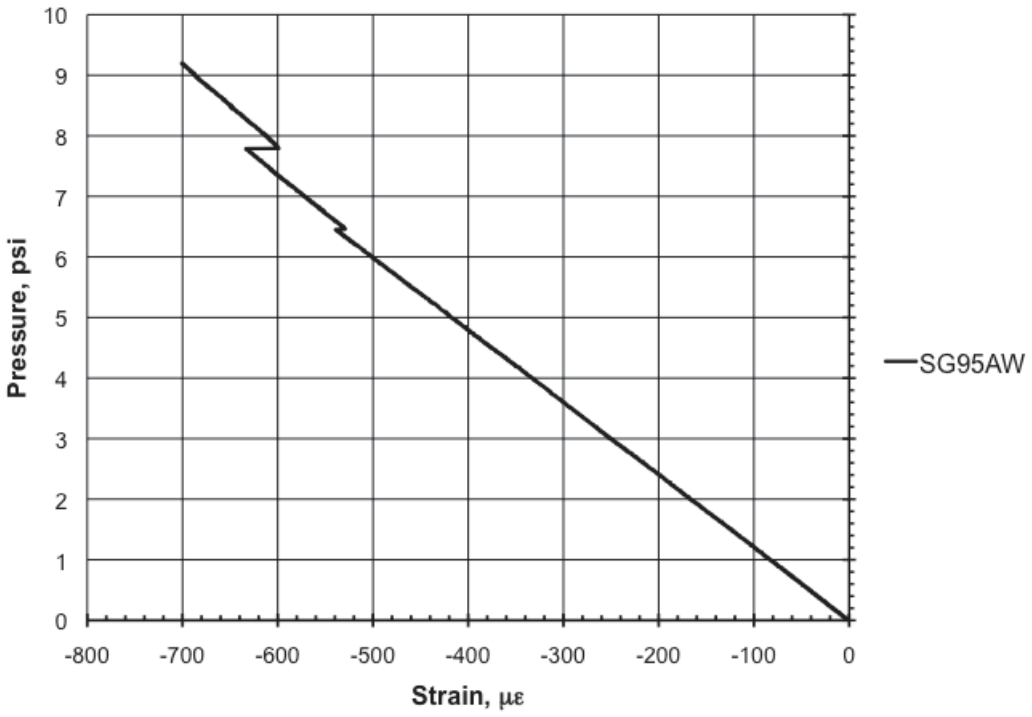

Figure 20. Strain recorded by gage SG95AW during loading up to 1P.

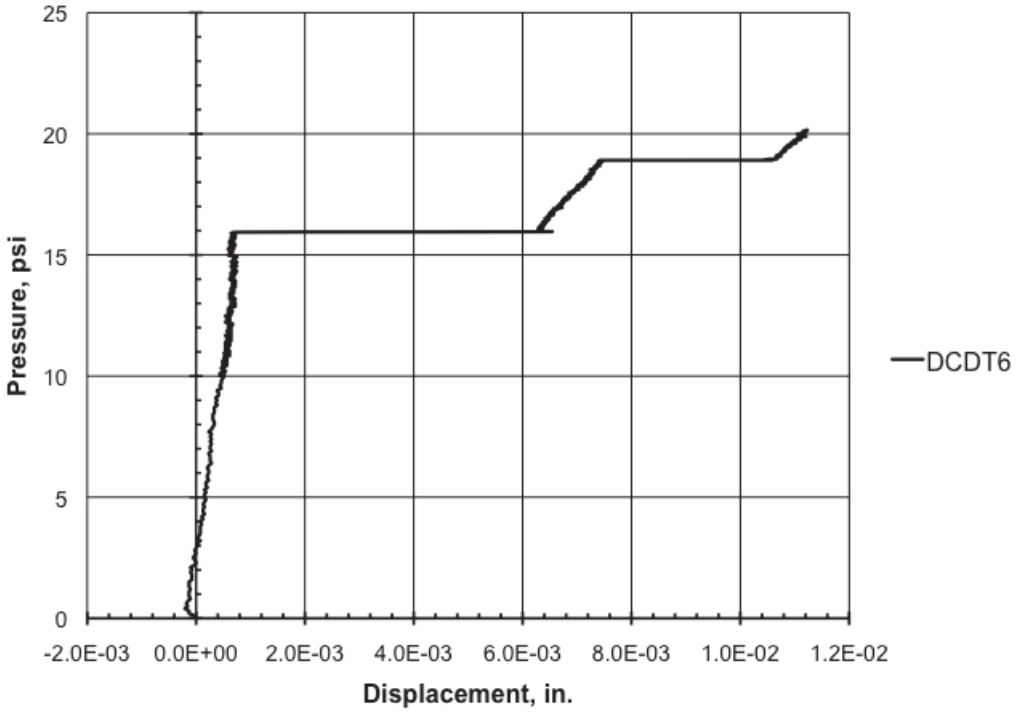

Figure 21. Displacement in DCDT6 for loading up to 2.2P.

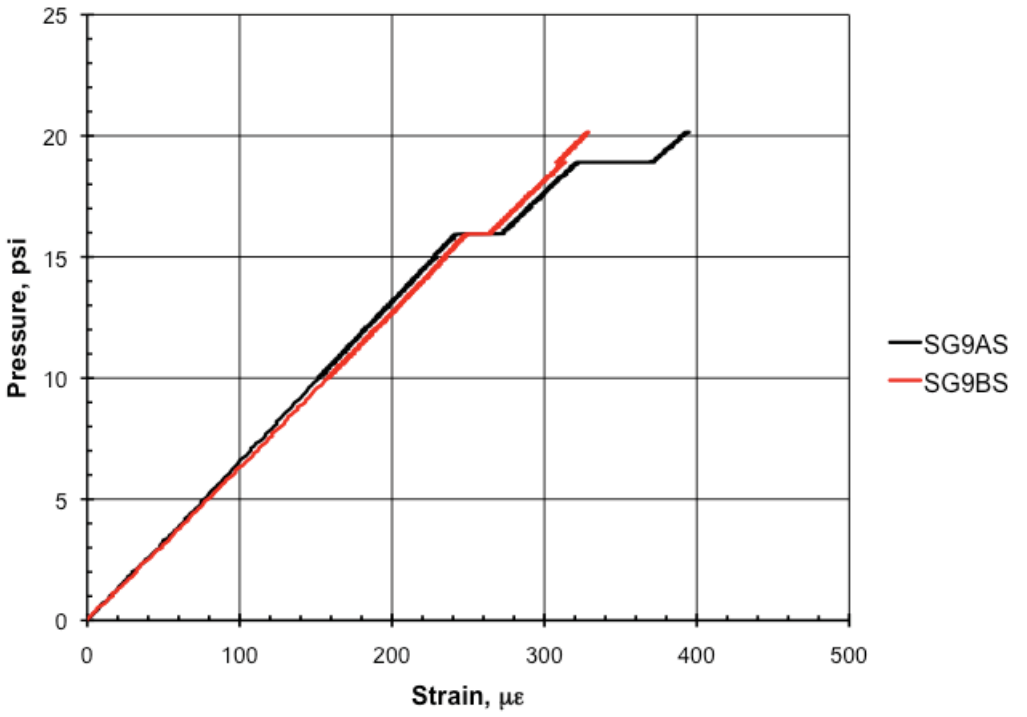

Figure 22. Strains recorded by gages SG9AS and SG9BS in loading up to 2.2P.

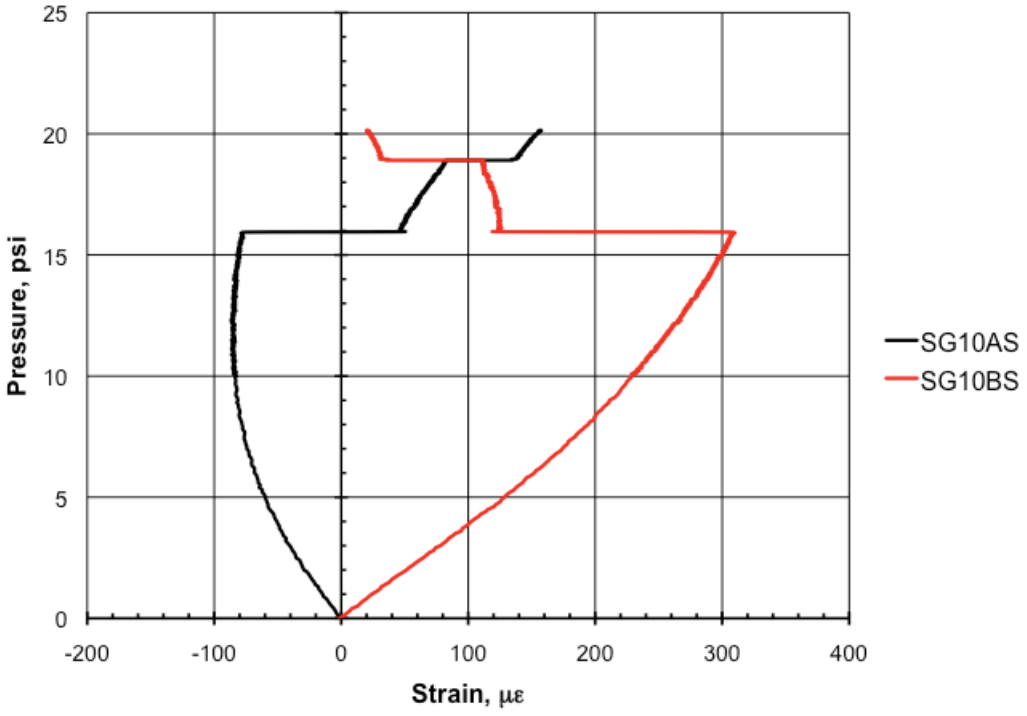

Figure 23. Strain recorded by gages SG10AS and SG10BS during loading up to 2.2P.

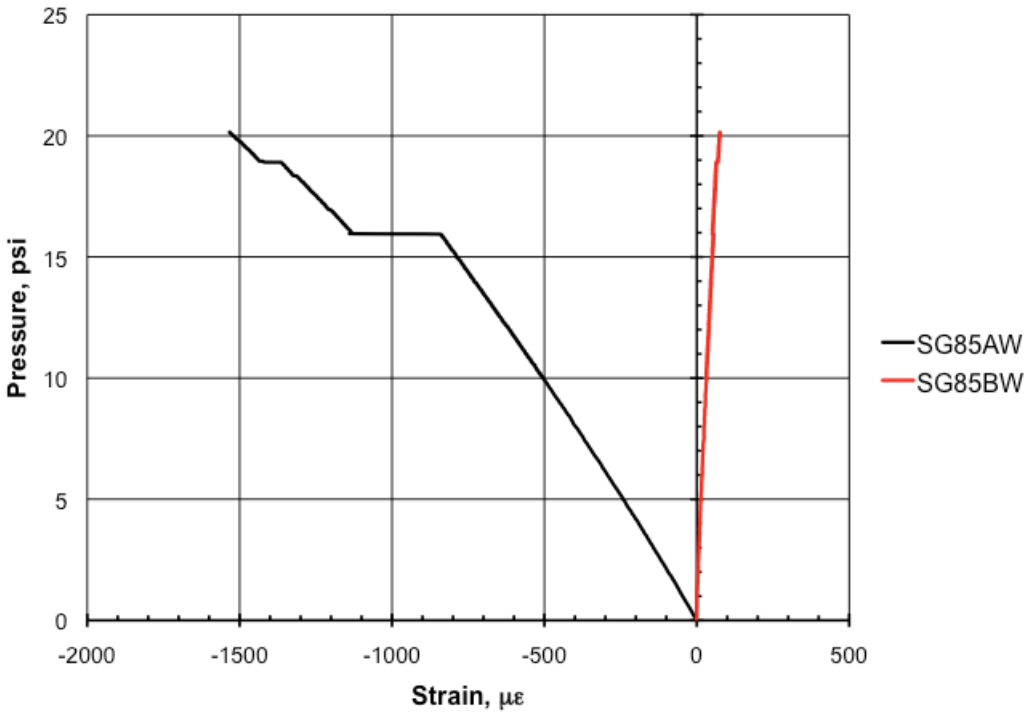

Figure 24. Strain recorded by gage SG85AW during loading up to 2.2P.

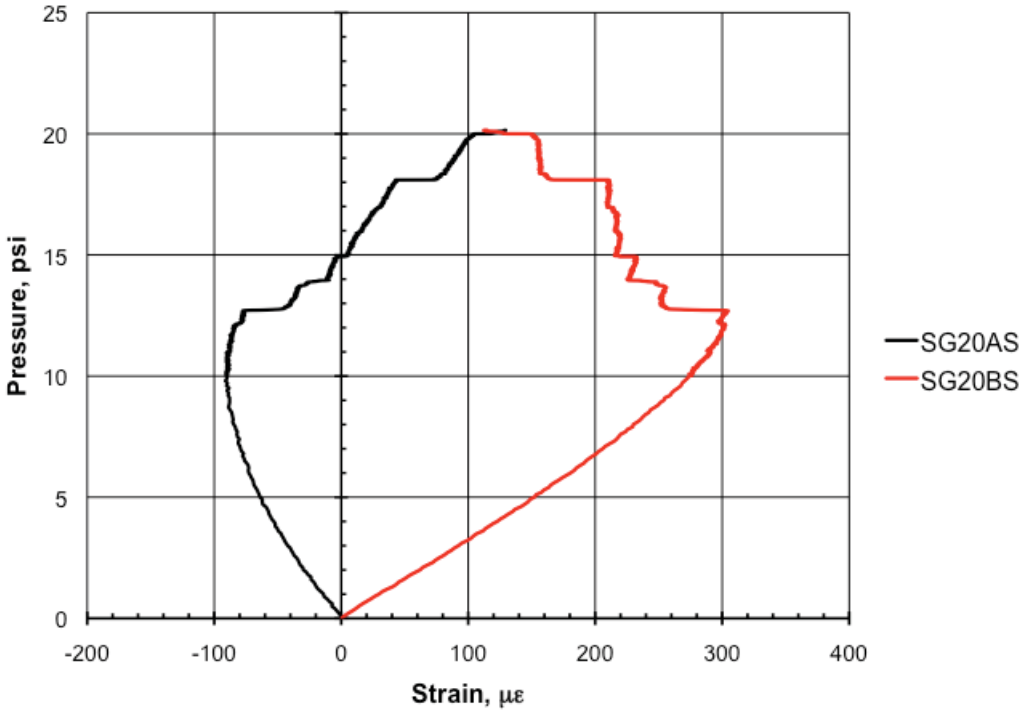

Figure 25. Strain recorded by gages SG20AS and SG20BS during loading up to 2.2P.

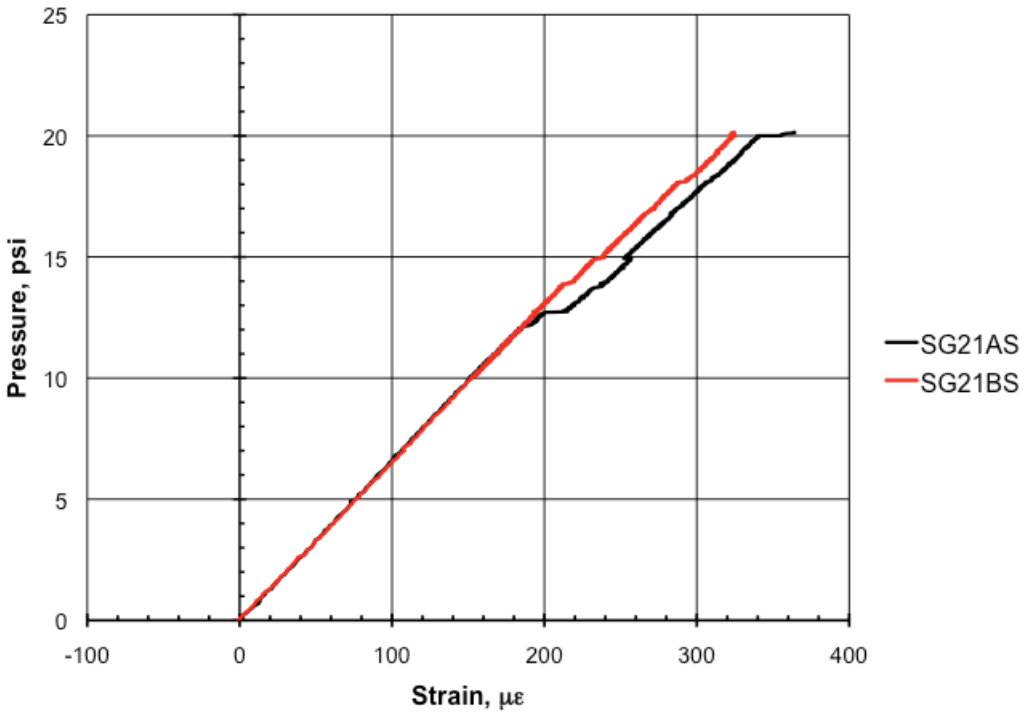

Figure 26. Strain recorded by gages SG21AS and SG21BS during loading up to 2.2P.

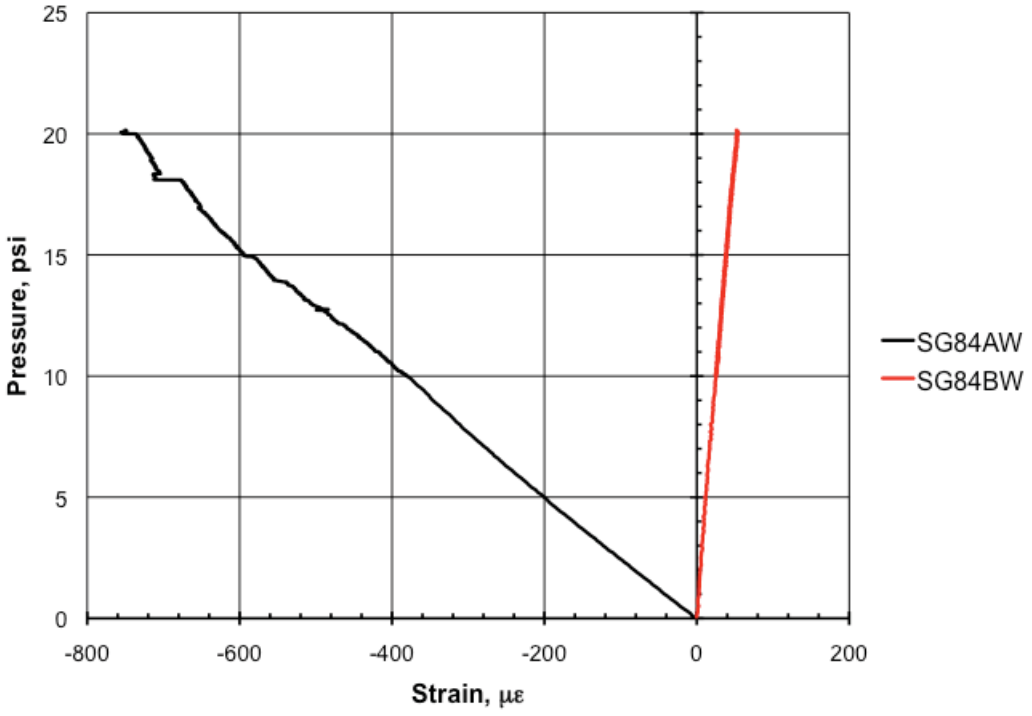

Figure 27. Strain recorded by gage SG84AW during loading up to 2.2P.

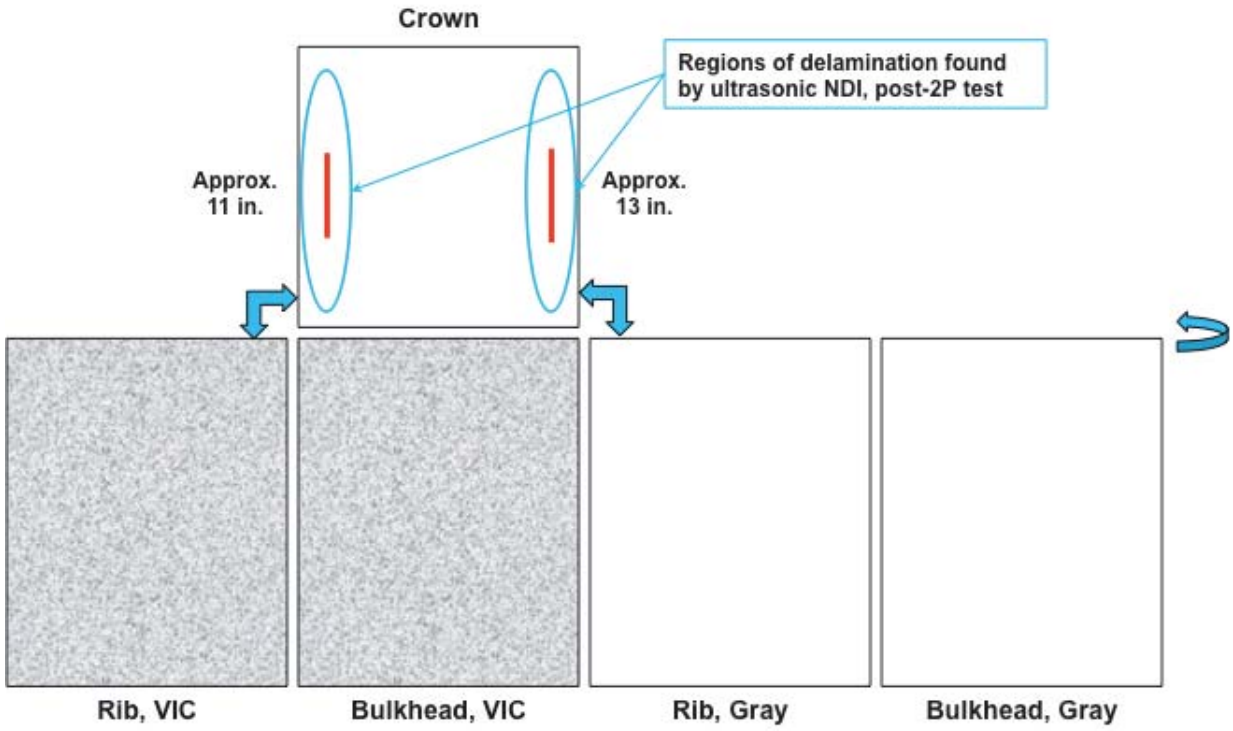

Figure 28. Delaminations discovered by NDI after loading up to 2.2P.

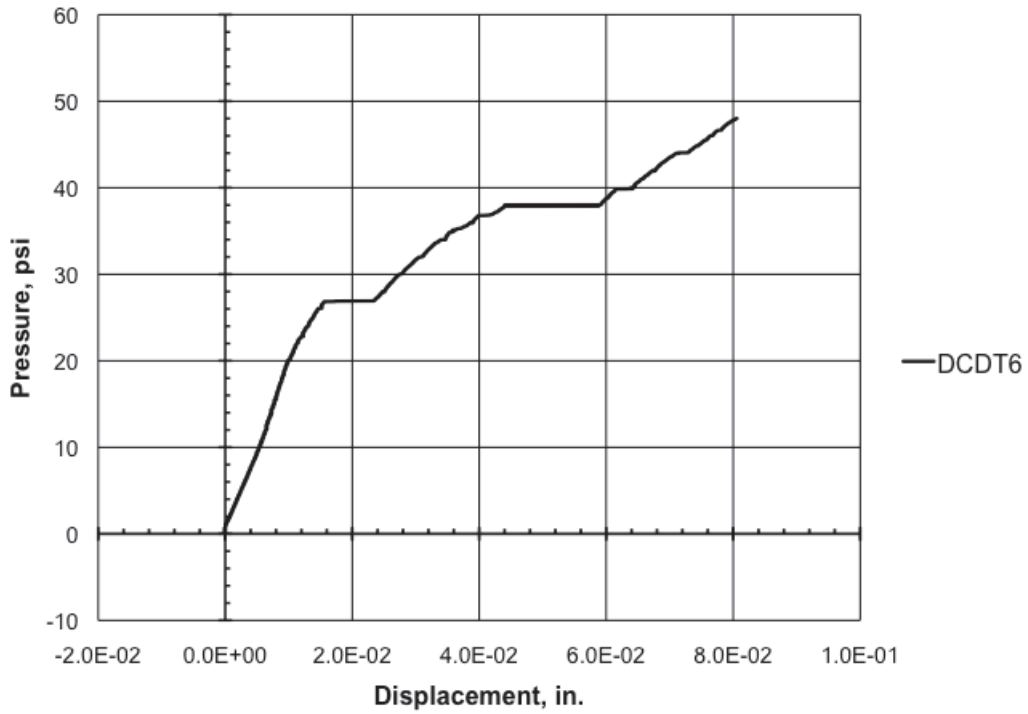

Figure 29. Displacement at DCDT6 during loading up to catastrophic failure.

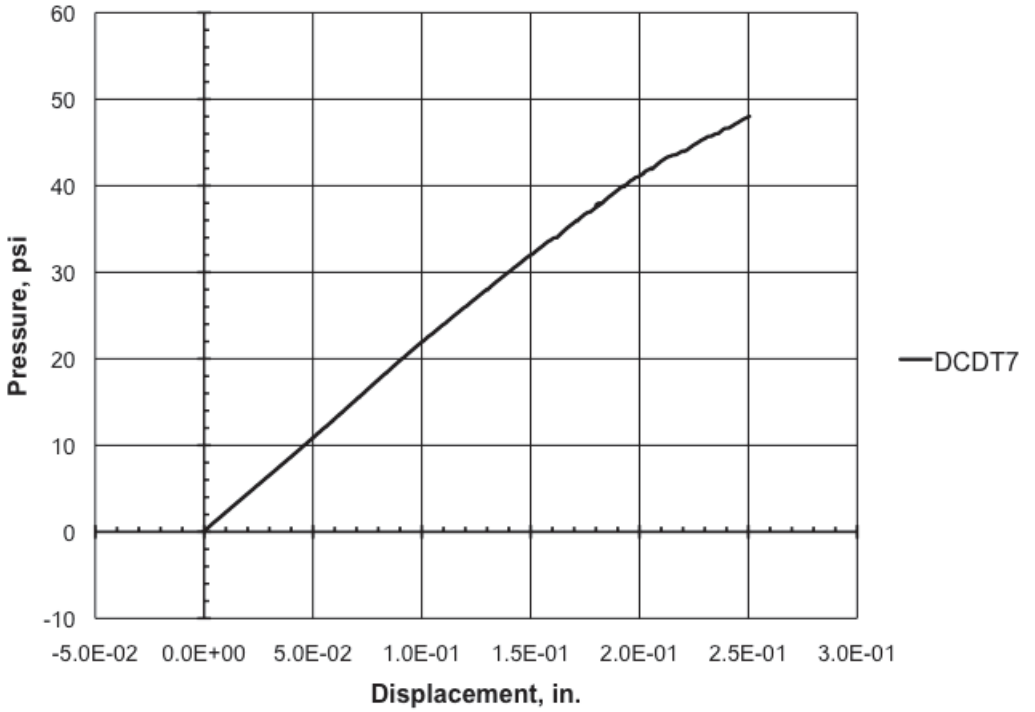

Figure 30. Displacement at DCDT7 for loading up to catastrophic failure.

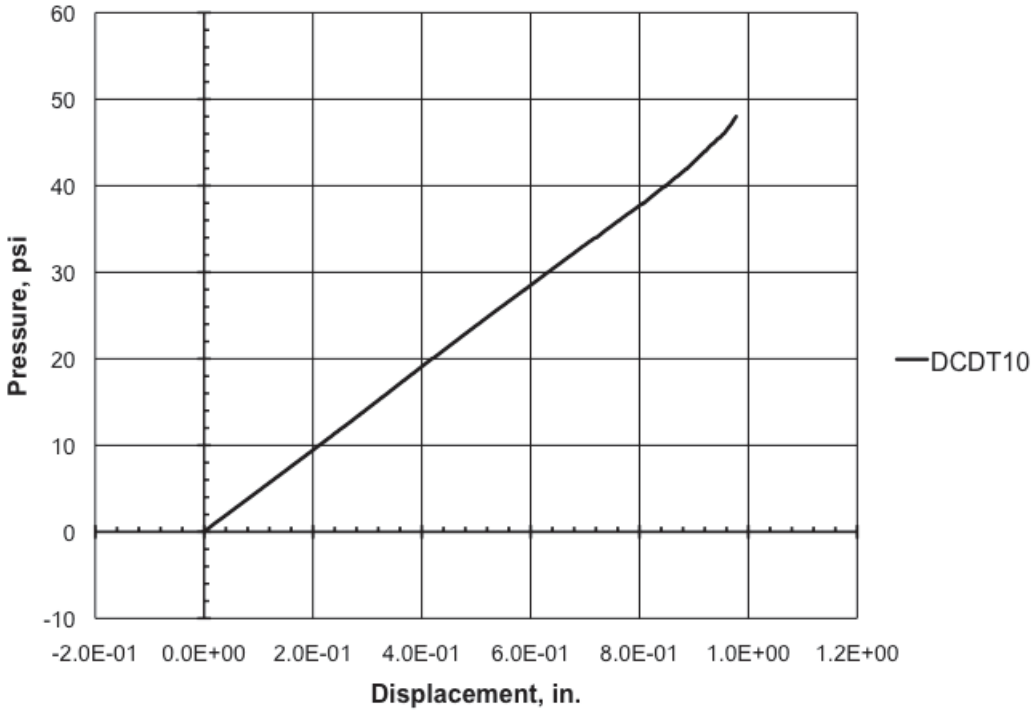

Figure 31. Displacement at DCDT10 for loading up to catastrophic failure.

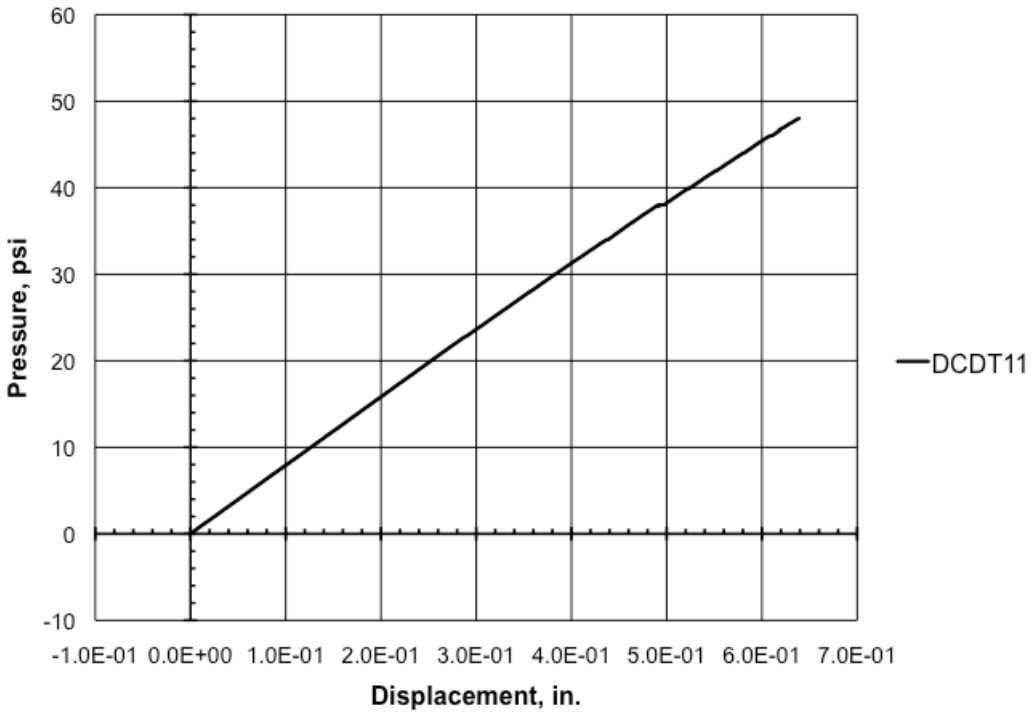

Figure 32. Displacement at DCDT11 for loading up to catastrophic failure.

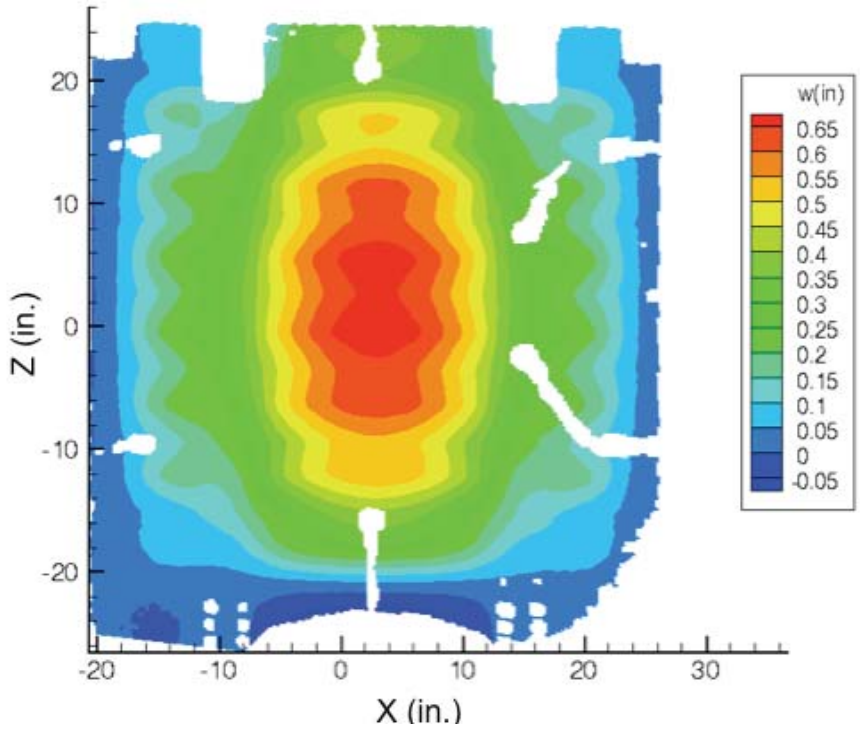

Figure 33. VIC normal displacement plot for rib just prior to catastrophic failure, approximately 48 psi. White space indicates area not recorded.

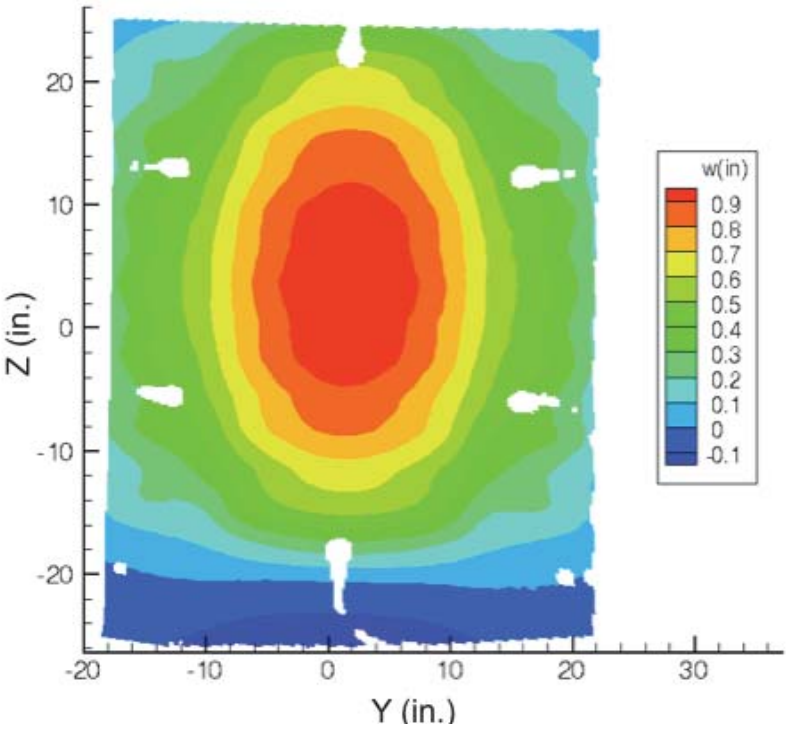

Figure 34. VIC normal displacement plot for bulkhead just prior to catastrophic failure, approximately 48 psi. White space indicates area not recorded.

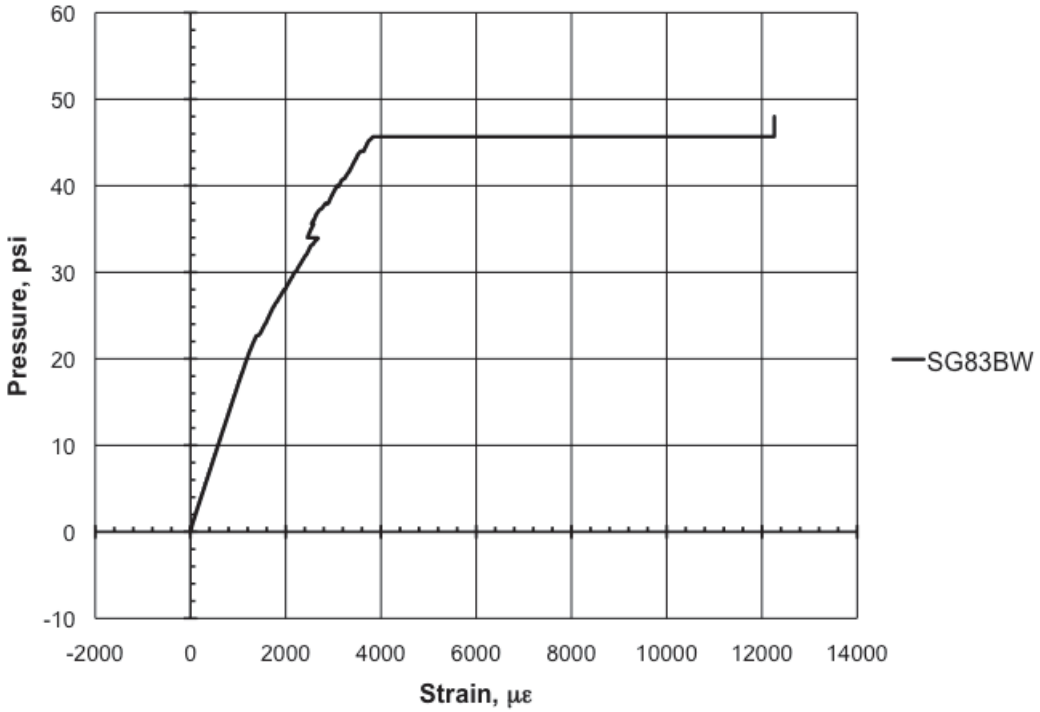

Figure 35. Strain measured at gage SG83BW during loading up to catastrophic failure.

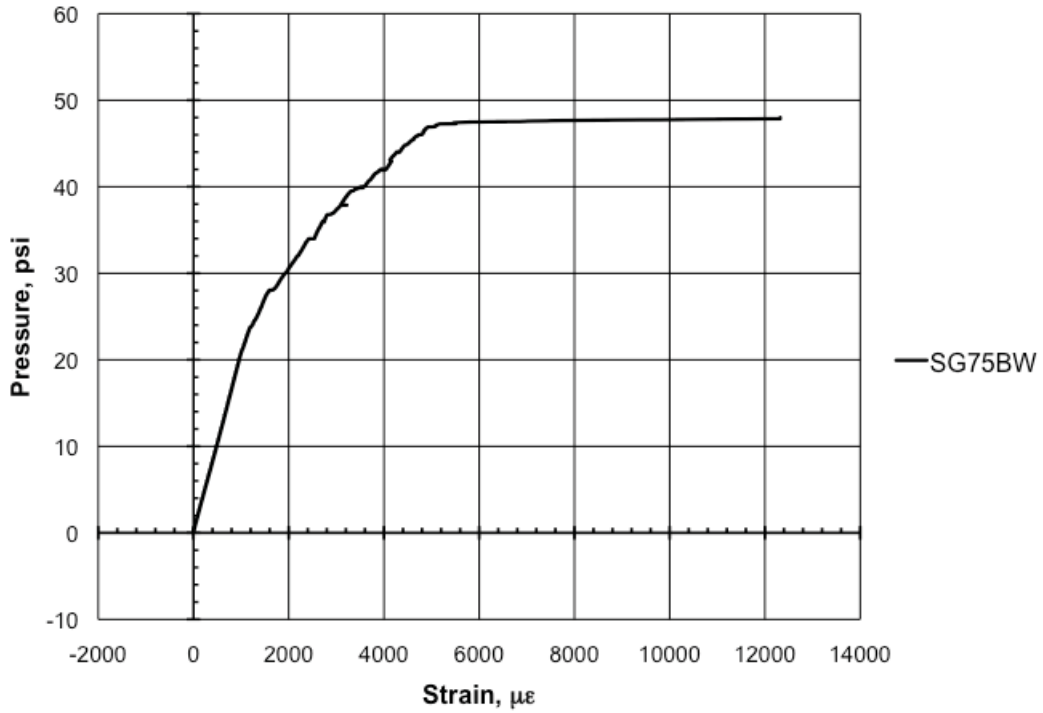

Figure 36. Strain measured at gage SG75BW during loading up to catastrophic failure.

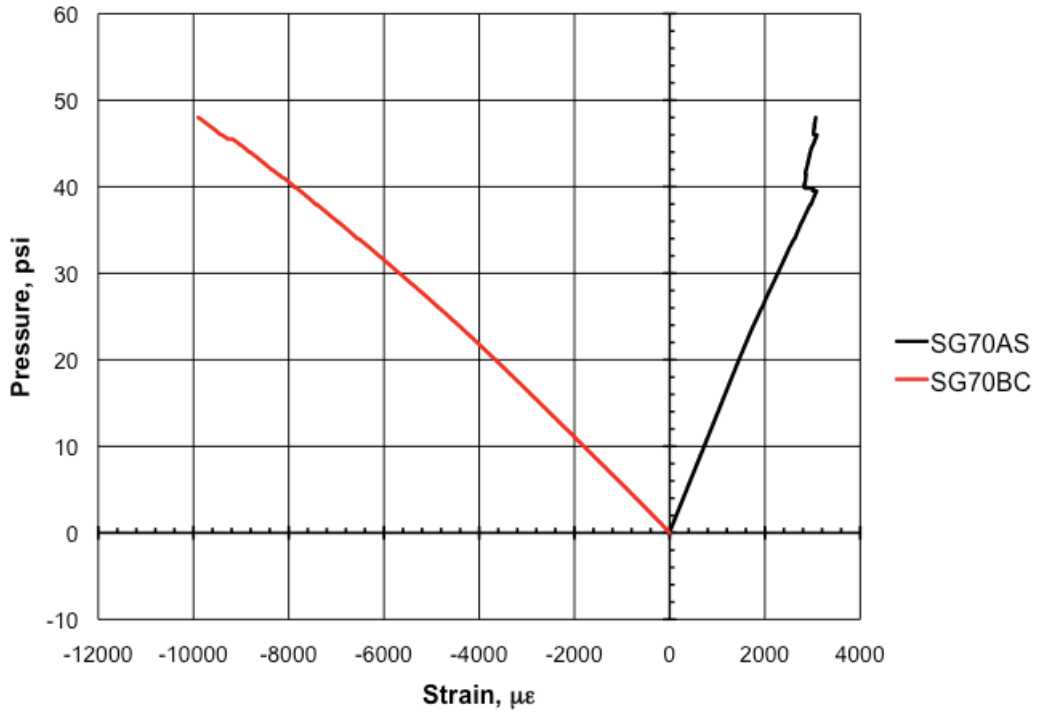

Figure 37. Strain measured at gages SG70AS and SG70BC during loading up to catastrophic failure.

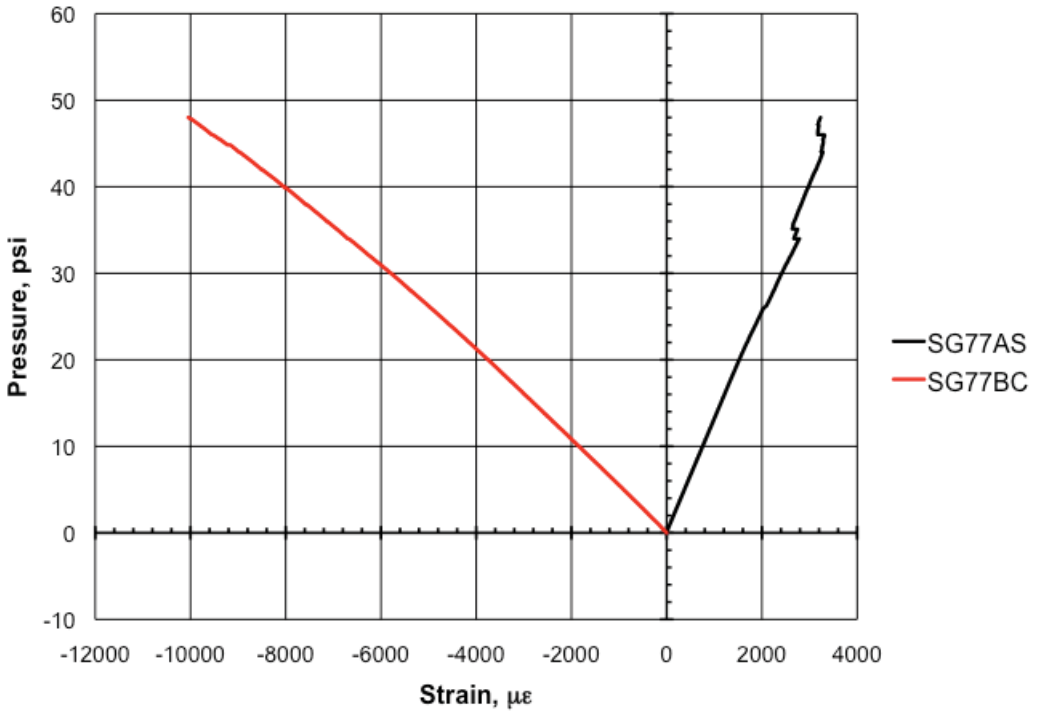

Figure 38. Strain measured at gages SG77AS and SG77BC during loading up to catastrophic failure.

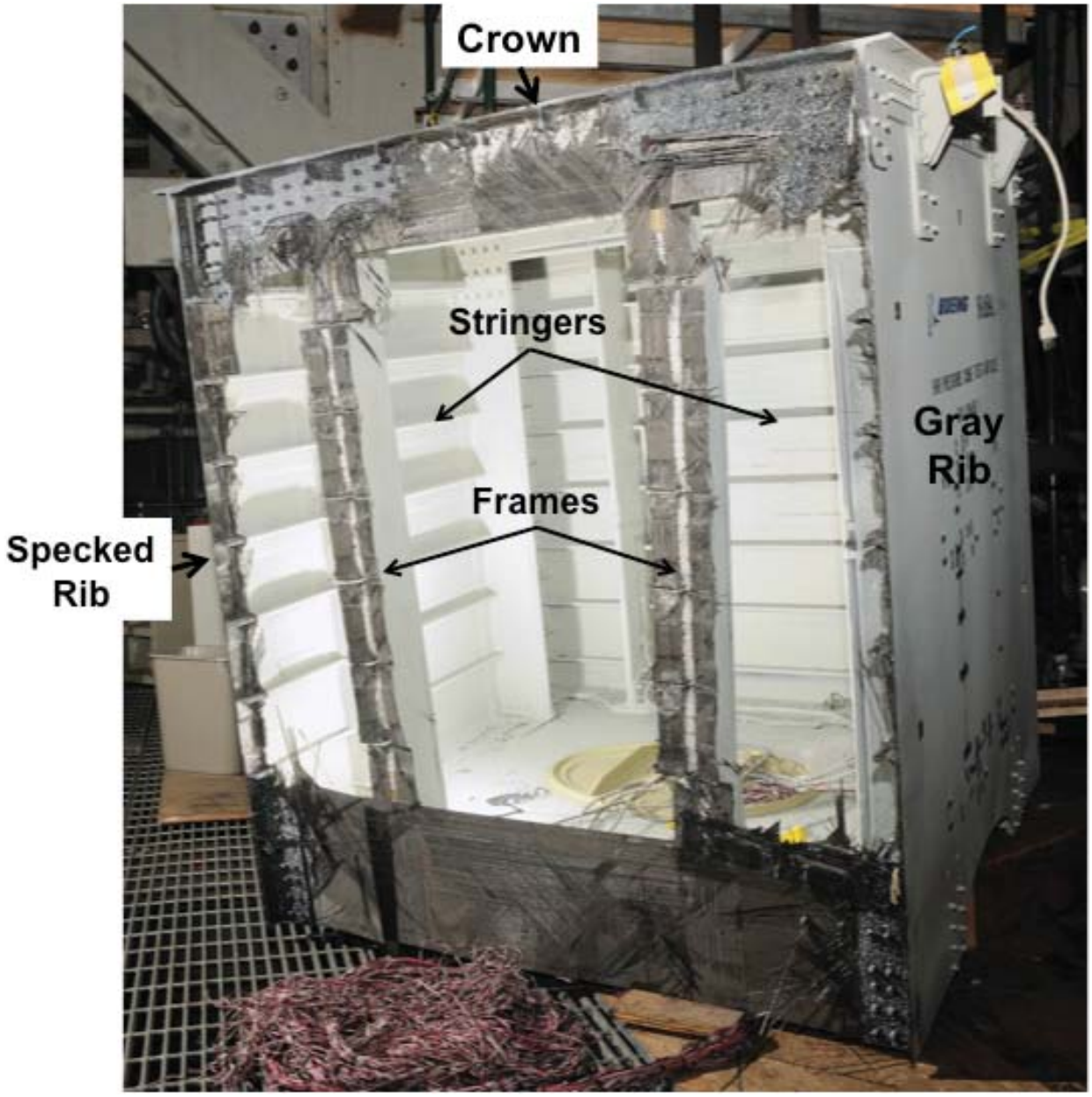

Figure 39. Failed pressure cube, VIC bulkhead panel blown off.

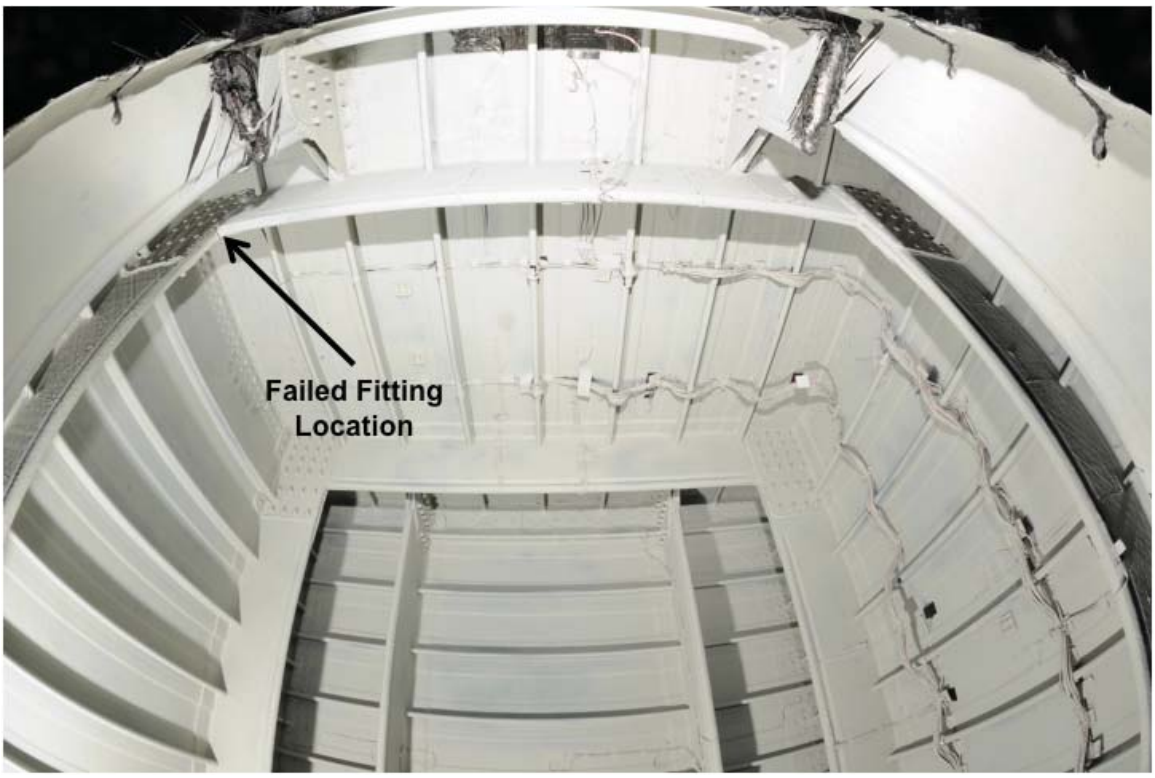

a) Location of failed fitting in cube, crown frame to VIC rib frame

b) Outside fitting

c) Inside fitting

Figure 40. Failed frame attachment fitting between crown and VIC rib in pressure cube.

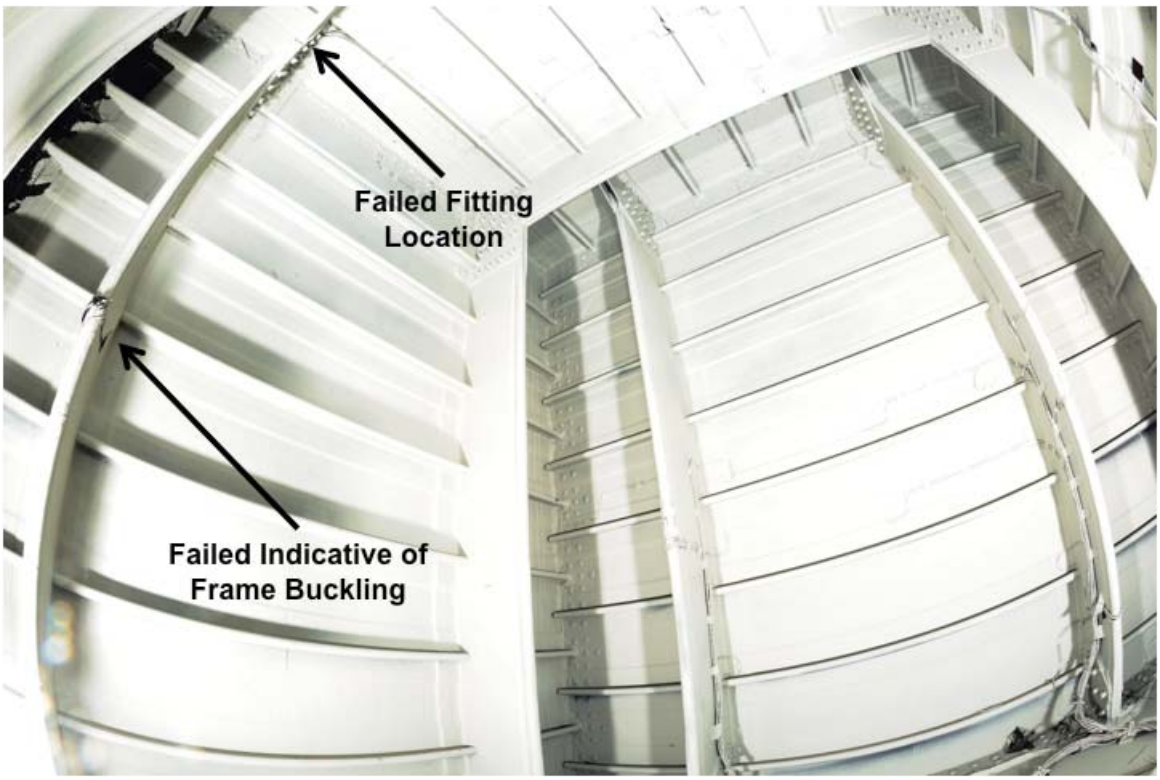

Figure 41. Indication of local buckling of rib frame attached to the failed frame fitting.